A process simulator interface for multiobjective optimization of chemical processes

Postprint version of paper published in Computers & Chemical Engineering 2018, vol.109, p. 119-137.
The content is identical to the published paper, but without the final typesetting by the publisher.

A process simulator interface for multiobjective optimization of chemical processes

Carlos André Muñoz López[a], Dries Telen[a], Philippe Nimmegeers[a], Lorenzo Cabianca[a], Filip Logist[a], Jan Van Impe[a,*]

[a] *KU Leuven, Chemical Engineering Department, BioTeC+ & OPTEC, Gebroeders De Smetstraat, 9000 Ghent, Belgium*

Abstract

The (bio)chemical process industry is under an increasing pressure due to smaller margins and increasing societal and legislative demands for a sustainable future. In this context model-based optimization contributes to the solution because it serves to improve the processes' performance. Furthermore, multiobjective optimization techniques provide the decision maker with a deeper insight in the tradeoffs when choosing an operating condition. However, an accurate process model is needed to apply these techniques efficiently. In this paper, a novel interface is developed between state-of-the-art gradient-based optimization techniques and the widely used process simulator Aspen Plus. Furthermore, specific challenges and solutions for overcoming the gap between process simulators and optimization tools are highlighted. The resulting interface allows gradient-based techniques to be exploited for optimization of complex industrial processes modeled in the advanced Aspen Plus environment. The interface ensures constraints satisfaction, and a higher computational performance than gradient free methods.

Keywords: Multiobjective optimization, Gradient-based optimization, Process optimization, Aspen Plus

1. Introduction

In light of the societal and legislative pressure on the process industry to increase its sustainability and to remain competitive in a more globalized world, model-based process optimization can play an important role both in process design and operation (Liu and Huang, 2012; Ren et al., 2016). When optimizing (bio)chemical

*Corresponding author
Email address: jan.vanimpe@kuleuven.be (Jan Van Impe)

Postprint of manuscript accepted for Computers and Chemical Engineering, January 26, 2018

Journal homepage: https://www.journals.elsevier.com/computers-and-chemical-engineering
Original file available at: https://www.sciencedirect.com/science/article/pii/S0098135417303198

processes, conflicting objectives are often present (Logist et al., 2009; Vallerio et al., 2015). A common example is the search for higher profitability while improving the safety of operation and reducing the energy consumption. However, the frequent influence of *inconmeasurable* parameters makes their numerical weighting into a single (economical) function practically infeasible. Therefore, a more informative approach is to provide the decision maker with a thorough view on the set of possible optimal solutions, in such a way that the sensitivity of the solutions and/or opportunity cost of the decision can be evaluated. Hence, the optimization methodology considered in this work is focused on dealing simultaneously with multiple and conflicting objectives, generating as result a set of possible solutions which offer the different tradeoffs between the objectives of interest.

Before model-based optimization can be performed, an accurate process model is required. For some applications this entails developing and executing costly experiments (Espie and Macchietto, 1989; Van Derlinden et al., 2010; Telen et al., 2014). In many process engineering approaches however this can be obtained by means of a process simulator. In this paper, Aspen Plus is considered as process simulator as it is widely used for the design and operation of chemical processes. However, it does not include advanced multiobjective optimization algorithms, which normally are able to generate valuable tradeoff knowledge of the investigated process models and can be expected to improve the process insight significantly. In the case of gradient-based optimization algorithms though, actual knowledge on the model equations is required, either the system of equations itself or sufficient information on the size, structure and gradient of the system, hence limiting its implementation to cases for which this information is available or can be formulated. This limitation motivates this work in which a connection between a widely used commercial process simulator and state-of-the-art gradient-based optimization techniques is established.

The solution of a multiobjective optimization (MOO) problem can be performed by a wide variety of algorithms. According to Ramzan and Witt (2006) the solution approaches can be divided in two: *ideal multiobjective optimization* procedures and *preference-based multiobjective optimization* procedures. This is equivalent to what

Journal homepage: `https://www.journals.elsevier.com/computers-and-chemical-engineering`
Original file available at: `https://www.sciencedirect.com/science/article/pii/S0098135417303198`

Logist et al. (2010) discuss when dividing the methods in vectorization and scalarization techniques. In both references the former case corresponds to methods that can directly tackle the MOO problem and produce at once a representation of the Pareto front. Information coming from the decision maker is then used to select one of the tradeoff solutions. Stochastic evolutionary algorithms, Genetic Algorithms (GA) and particle swarm optimization for multiple objectives are examples of these methods (Rangaiah and Bonilla-Petricolet, 2013). The latter case on the other hand corresponds to methods which reformulate the MOO into one or multiple parametric single objective problems to solve them individually.

Rangaiah and Bonilla-Petricolet (2013) subclassify the scalarization methods depending on two features: the introduction of the decision maker's preferences and the possibility to obtain one or multiple solutions. Classical scalarization methods which require *a priori* decision maker's information, produce only one non-dominated solution. If multiple solutions are desired, it is required to program a sequence of different problems with different values for the parameters. Some examples of the former category are the weighted methods (e.g., global criterion, weighted sum, weighted min-max, weighted product, exponential weighted), ε-constraint and the goal programming methods (Miettinen, 1999). In contrast, examples of the latter are Normal Boundary Intersection (NBI) (Das and Dennis, 1998) and Normalized Normal Constraint (NNC) (Messac et al., 2003) where the preference is articulated *a posteriori* or interactively(Logist et al., 2010; Vallerio et al., 2015).

In this contribution, some selected methods for the vectorization and scalarization approaches are applied. The aim is to compare their performance on the process simulator interface using a debutanizer column model as an illustrative case study, and to highlight the advantages of the proposed gradient-based approach using the scalarization methods. Some of these advantages are a better performance in terms of computational time and a higher accuracy to tackle constrained problems (Logist et al., 2013). In the last part the interface using scalarization methods is exploited for the optimization of two industrially relevant case studies, the butyl acetate production process and the methanol production via methane tri-reforming.

Journal homepage: `https://www.journals.elsevier.com/computers-and-chemical-engineering`
Original file available at: `https://www.sciencedirect.com/science/article/pii/S0098135417303198`

Enabling MOO in a process simulator is not straightforward. The most common approach found in literature employs *black box optimization* which does not require model information. This type of interfaces between the process simulator and the optimization algorithm are built to transfer model evaluation values (dependent variables) and the iterative values of the decision variables (independent variables). In this direction, Diwekar et al. (1992) proposed a Mixed Integer Nonlinear Programming (MINLP) synthesizer using Aspen Plus through a stochastic annealing algorithm. Tarafder et al. (2005) implement NSGA-II (Deb et al., 2002) to apply MOO of a simulated industrial styrene monomer manufacturing process. Jang et al. (2005) developed and hybrid genetic algorithm that introduces a quadratic search in a region defined after some generations of the GA, and coupled it to Aspen Plus. Gutierrez and Briones (2009) use NSGA-II in the MOO of a rigorous model for Petlyuk sequences in Aspen Plus. Similarly Bravo et al. (2010) use GA in the design and optimization of a Extractive Dividing Wall Column. Eslick et al. (2011) present a framework for the MOO of processes using Aspen Plus models, Excel and modeFRONTIER, where the optimization algorithm is NSGA-II. Taras and Woinaroschy (2012) use NIMBUS algorithm (Miettinen, 1999) and a GA in an interactive MOO framework, interfacing SuperPro Designer and Matlab. Finally, Wang and Feng (2013) optimize the hydrogen production in a refinery modeled in Aspen Plus using NSGA-II.

In contrast, to exploit gradient-based optimization algorithms, either the set of model equations is made available or sufficient gradient information is provided directly to the solver. Only few cases are found to be based on the availability of the model equations. Hakanen et al. (2006) developed an integrated multiobjective design tool for process design using BALAS which is a steady state simulation package for chemical processes with emphasis on pulp and paper processes. Bortz et al. (2014) propose a scheme for MOO acquiring the required model information from the available source code of CHEMASIM which is an equation oriented steady-state flowsheet simulator developed by BASF SE. On the contrary, most of the flowsheet simulators do not make the system of model equations available. Therefore, differ-

Journal homepage: `https://www.journals.elsevier.com/computers-and-chemical-engineering`
Original file available at: `https://www.sciencedirect.com/science/article/pii/S0098135417303198`

ent approaches have been investigated to provide the gradient information to the Nonlinear Programming (NLP) solvers. Harsh et al. (1989) exploited the derivative information available from an optimization problem formulated in FLOWTRAN to interface it with a Mixed-Integer Nonlinear Programming (MINLP) algorithm and accomplish the retrofit of an ammonia process. Diaz and Bandoni (1996) proposed, using the same flowsheet simulator, to estimate numerically the gradient information by finite differences and using it in the MINLP formulation for the optimization of an ethylene plant. Based as well in numerical estimation of the gradient information, Navarro-Amoros et al. (2014) introduce a framework for integrating chemical process simulators, explicit equations and third party models with gradient based optimization.

A slightly different approach is the use of the *equation set object* (ESO). This approach relies on interfacing a set of information (e.g., gradient and variable information) which is defined according to CAPE-OPEN standards (Lang and Biegler, 2007). This interface allows access to the structure of the model (i.e., the number of variables and equations, and the sparsity pattern of the Jacobian), as well as to information on the involved variables (i.e., their names, current values, and lower and upper bounds) (Leineweber et al., 2003). Some examples are presented by Leineweber et al. (2003) at optimizing dynamic processes using MUSCOD-II and by Lang and Biegler (2007) whom developed the software tool DynoPC to optimize dynamic processes modeled in gPROPMS.

Alternatively to process simulators that support the CAPE-OPEN standard, other simulator packages have developed equivalent strategies to be interfaced with optimization algorithms. In Chen et al. (2009) an IPOPT based solver and CAPE-OPEN solvers were encapsulated and embedded into the *Aspen custom modeler* via the Aspen Open Solvers (AOS) interface using Dynamic Link Libraries (.dll files). This shows that the AOS interface supports similar operations to the ESO interface. However, in the case of the AOS interface, the model information is not handled out of the process simulator but the optimization algorithm is embedded into the simulation instead, reducing significantly the flexibility of the interface and

Journal homepage: `https://www.journals.elsevier.com/computers-and-chemical-engineering`
Original file available at: `https://www.sciencedirect.com/science/article/pii/S0098135417303198`

making it less accessible. Alternatively to the AOS approach, the Open Object Model Framework (OOMF) included within the AspenTech software packages offers programmatic access to the equation-oriented engine (Aspen, 2011). In this contribution the OOMF is exploited to develop an interface with similar capabilities to an CAPE-OPEN ESO interface for Aspen Plus. This interface allows the connection of Aspen Plus to gradient-based MOO methods, such that Pareto optimal points can be computed more efficiently using gradient information from the model that has been computed analytically by the Equation Oriented (EO) engine. Furthermore, the specific challenges and solution approaches for the use of process simulator models in optimization tools are highlighted. This contribution is expected to provide users with an increased insight in the process operation and allow for a more informed decision.

The paper is structured as follows. Section 2 introduces the mathematical formulation of MOO and describes the employed methods. In section 3, the strategy and the developed interface are discussed, it covers aspects on the optimization tool and the process simulator Aspen Plus. The description of the three considered case studies is provided in section 4. The obtained numerical results are presented and discussed in section 5. The conclusions are summarized in the final section of the paper.

2. Multiobjective optimization

In this section the mathematical formulation of the considered MOO problems is presented. Subsequently the employed MOO techniques are discussed.

2.1. Mathematical formulation

Multiobjective optimization (MOO) refers to the simultaneous optimization of two or more objective functions which are typically conflicting. In practice this means that by improving one of the objectives another is worsened. The formulation of a MOO problem considered in this paper is given by:

Journal homepage: `https://www.journals.elsevier.com/computers-and-chemical-engineering`
Original file available at: `https://www.sciencedirect.com/science/article/pii/S0098135417303198`

$$\min_{\mathbf{u}\in R^{n_u}} [J_1(\mathbf{x},\mathbf{u}),\ldots,J_n(\mathbf{x},\mathbf{u})] \tag{1a}$$

subject to:

$$\mathbf{0} \geq \mathbf{g}(\mathbf{x},\mathbf{u}) \tag{1b}$$

$$\mathbf{b}_l < \mathbf{u} < \mathbf{b}_u \tag{1c}$$

$$\text{with: } \mathbf{y} = [\mathbf{u}^\top, \mathbf{x}^\top]^\top \tag{1d}$$

In this formulation $\mathbf{J} \in R^n$ is the set of objective functions defined by independent variables (controls) $\mathbf{u} \in R^{n_u}$ and dependent variables (states) $\mathbf{x} \in R^{n_x}$. The relation between the two set of variables is given by a fully determined system of model equations $0 = \mathbf{f}(\mathbf{x},\mathbf{u})$ with $\mathbf{f} \in R^{n_x}$. These are the flowsheet equations solved independently by the process simulator and they represent e.g., thermodynamics, mass and energy balances and reaction kinetics. The vector $\mathbf{y}$ is used in view of conciseness to represent the set of variables with a total number of variables $n_y = n_x + n_u$. The vector $\mathbf{g}$ denotes the n_c equality and inequality constraints of the problem. Additionally, in this formulation the lower ($\mathbf{b}_l$) and upper bounds ($\mathbf{b}_u$) for the independent variables are explicitly established as boundary constraints (Rangaiah and Bonilla-Petricolet, 2013).

The *feasible space* Ω of the optimization problem is defined as the set of vectors $\mathbf{y}$ which satisfy all the constraints and bounds set in Equations (1b), (1c) and (1d). The difference between *single objective optimization* (SOO) and *multiobjective optimization* (MOO), is that finding a unique vector $\mathbf{y}$ which optimizes simultaneously all conflicting objectives is not possible. Consequently for a MOO problem a set of vectors $\mathbf{y}^*$ is found as *Pareto-optimal*. A point $\mathbf{y}^* \in \Omega$, is Pareto optimal iff there does not exist another point, $\mathbf{y} \in \Omega$, such that $J_j(\mathbf{y}) \leq J_j(\mathbf{y}^*)$ for all $j \in 1,...,n$ and $J_i(\mathbf{y}) < J_i(\mathbf{y}^*)$ for at least one objective function i (Vallerio et al., 2015).

The solution of a MOO problem and the construction of its Pareto front can be perform following two approaches (Logist et al., 2010): vectorization and scalarization methods.

Journal homepage: `https://www.journals.elsevier.com/computers-and-chemical-engineering`
Original file available at: `https://www.sciencedirect.com/science/article/pii/S0098135417303198`

2.2. Scalarization methods

Scalarization methods transform the multiple objective optimization problem (MOOP) into a (series of) parametric single objective optimization problems. Therefore, they do not tackle directly the whole MOOP but they still can produce multiple non-dominated results by solving the parametric single problems sequentially. Additionally, since these methods often exploit deterministic gradient-based optimization approaches they tend to be fast and are able to account efficiently for constraints both on decision variables as well as dependent variables (Logist et al., 2010, 2013).

In this contribution two scalarization methods are implemented, the Normal Boundary intersection (NBI) and the Normalized Normal contraint (NNC). These methods are able to cope with the intrinsic drawbacks of the simpler *a priori* scalarization methods (e.g., weighted sum, and ε-constraint). They produce a uniform spread of points on the Pareto front, covering non-convex segments as well, and the solution is independent of the objectives' scale (Logist et al., 2010).

These two methods are based on a geometric approach of the objective function space. The *anchor points* i.e., the individual minimization of each of the different objectives, are determined first, subsequently a convex combination is used to reformulate the problem following two different approaches. NBI (Das and Dennis, 1998) searches for the Pareto optimal points over (quasi-)normal lines to the convex combination plane, looking for the points in the feasible objective space that are closest to the *utopia point*, i.e., the point consisting of all the individual minima. Meanwhile NNC (Messac et al., 2003) looks for optimal solutions for one of the original objectives but in a reduced version of the feasible space. This is constrained by *normal hyperplanes* based on the remaining objective functions. The detailed formulation and description of the resulting optimization problems can be found in Logist et al. (2010).

2.3. Vectorization methods

Vectorization methods are typically based on stochastic search procedures by sequential evaluations of the objective functions. The main feature is the ability to

Journal homepage: `https://www.journals.elsevier.com/computers-and-chemical-engineering`
Original file available at: `https://www.sciencedirect.com/science/article/pii/S0098135417303198`

tackle directly the MOO problem and to produce multiple non-dominated results simultaneously. Additionally, they are considered as easy to implement, flexible to be coupled with process simulators and generally regarded as global optimization approaches (Logist et al., 2010). The higher capability of these methods to determine global optimal solutions is mainly based on random search with multiple sampling in the feasible space and it is improved if multiple non-dominated individuals are kept simultaneously so the chances are higher for finding a path that leads to a global solution. The model is treated as a black box and therefore model information is not required (Bortz et al., 2014). Specifically, the elitist Nondominant Sorting Genetic Algorithm (NSGA-II) (Deb et al., 2002) is frequently used for solving many chemical engineering applications. The NSGA-II method is chosen as the vectorization approach to solve MOO problems in this contribution.

NSGA-II is an improved version of the NSGA algorithm (Srinivas and Deb, 1994). It is an evolutionary algorithm (EA) based on a multiobjective genetic algorithm. It follows the Goldberg ranking method (Goldberg, 1989) in the fitness assignment and evaluation, which is based on the Pareto optimality or Pareto ordering. Furthermore, NSGA-II uses the *crowded distance* and the *crowded tournament selection* strategies to preserve the diversity among solutions in the Pareto front while it preserves non-dominated individuals found at intermediate generations (Nakayama et al., 2009).

3. The interface between a process simulator and an optimization tool

In this section the developed interfaces linking the process simulator to the optimization tool are discussed. The first interface is for the black box optimization approach while the second one is aimed at gradient-based optimization by accessing the so-called *equation set object*. Detailed information is presented on how the complete simulation-optimization scheme is implemented. First, the description of the employed software tools is presented. Subsequently, the requirements of the interface and the proposed solution are discussed.

Journal homepage: https://www.journals.elsevier.com/computers-and-chemical-engineering
Original file available at: https://www.sciencedirect.com/science/article/pii/S0098135417303198

3.1. Software tools

Matlab R2014b is used as optimization platform. It allows to implement a wide variety of optimization algorithms, using embedded functions, as part of the optimization toolbox, or scripted by the user. This contribution aims to compare the vectorization and scalarization approaches, and Matlab offers the required flexibility to implement multiple optimization algorithms. On the one hand, the NSGA-II method is employed via Matlab's function *gamultiobj*. This is a variant of NSGA-II created to run on Matlab's environment (Bau et al., 2015). On the other hand, algorithms for NBI and NNC are scripted in the CasADi environment. CasADi is a symbolic framework for automatic differentiation and numerical optimization (Andersson et al., 2012), which additionally provides an interior point method (IPOPT (Wächter and Biegler, 2006)) to solve the resulting NLP problems. Finally, Aspen Plus is used as process simulator, it offers EO mode (Apen, 2005), which guarantees handling gradient information of the model equations.

IPOPT is exploited along this work to solve the NLPs resulting from the application of the NBI and NNC methods to the MOOPs. This method is based on the application of the interior point method or *barrier method* to solve inequality constraints. Line search methods are applied for the solution of the IPOPT problem, therefore gradient information is needed. In this work a low rank update based on the BFGS scheme is used (Nocedal and Stephen, 1999), because the exact Hessian is not available.

3.2. Interface description

Three different approaches are identified for interfacing process simulators and optimization algorithms, i.e., *black box optimization*, *access to the equation set object* and *access to the set of model equations*. The main difference between the three approaches is what information is transferred to the external optimization tool.

Black box optimization: This is a well-known and often exploited approach for interfacing a process simulator and complex stochastic optimization algorithms (e.g., Aspen Plus and NSGA-II being executed on Matlab or Visual basic). This approach is based on exploiting the information contained in successive objective

Journal homepage: https://www.journals.elsevier.com/computers-and-chemical-engineering
Original file available at: https://www.sciencedirect.com/science/article/pii/S0098135417303198

function evaluations since the model remains unknown. There exist several references based on this approach. For example, Gerali and Romagnoli (2015) present an optimization framework using a multiobjective stochastic optimization approach to incorporate tradeoffs between cost and financial risk for the design of integrated biorefineries. However, there are limitations in applying this approach. For example in the case of using NSGA-II, it has been reported that the performance decreases if other constraints than simple bounds for the decision variables are included (Logist et al., 2013). In this work black box optimization will be implemented for comparison.

Access to equation set object (ESO): This approach refers to implementing the ESO interface defined according to CAPE-OPEN standards. This is transferring a set of information derived from the model but not the model equations. The set of information is defined as the minimum required to execute gradient-based optimization algorithms. Different from the identified references following this approach Leineweber et al. (2003), Schopfer et al. (2005), Lang and Biegler (2005), Lang and Biegler (2007), which all used *gProms*, Aspen Plus does not support this standard. Therefore the approach presented in this contribution exploits OOMF to get programmatic access to the equation oriented engine and querying the same minimal information provided by an ESO interface. Taking advantage of this feature, an ESO equivalent interface is constructed to link Aspen Plus and Matlab. This interface has the capability of efficiently exploiting gradient-based optimization algorithms.

Access to the set of model equations: This approach is the ideal approach from an optimization point of view. It could require a single interaction between process simulator and optimizer, i.e., the transfer of the set of model equations. Therefore, this approach can result in a high performance. Unfortunately it is limited by the typically constrained access to model equations in process simulators. Only few cases exist in the literature following this approach. In Sadrieh and Bahri (2011) an implementation is presented using models from Aspen Plus via Aspen Custom Modeller (ACM). However, this is a highly complex procedure that re-

Journal homepage: https://www.journals.elsevier.com/computers-and-chemical-engineering
Original file available at: https://www.sciencedirect.com/science/article/pii/S0098135417303198

quires additional program utilities to interpret the process model and to integrate the complete implementation into ACM. Therefore, limiting the applicability and iteration with the optimization solver. Consequently this approach has not been followed in this work.

3.3. Interface architecture

The conceptual architecture for the developed interface of this contribution is the result of four components, i.e., the simulation software, the middleware, the wrapper protocol and the optimization platform. Figure 1 represents this structure graphically, where the interface is strictly formed by the middleware and the wrapper protocol (dashed line). On the one hand the middleware protocol is implemented to allow partial automation of the process simulator and to transfer in both directions the required information. Some middleware protocols are ActiveX(COM) and CORBA. On the other hand the employed wrapper protocol serves to interpret the information transferred by the middleware and transform it on useful information that can be exploited either by the optimization algorithm or simulator.

The type of optimization to be performed, i.e., either black box or accessing the ESO, determines what type of information needs to be transferred and which interactions have to be enabled between the process simulator and the optimization platform. In case of black box optimization, it consists of only the values of the dependent and independent variables for which read and writing actions should be allowed. In contrast when gradient-based optimization is aimed at, more complex information structures and actions have to be considered. The ESO CAPE-OPEN standard is used as reference to define what should be considered on the interface (CO-LaN, 2003):

- Obtain the current values of a specified subset of the variables (controls and states).
- Alter the values of any specified subset of the independent variables (controls).
- Get the structure of the sparse matrix representing the partial derivatives of a specified subset of the equations with respect to a specified subset of the variables.

Journal homepage: `https://www.journals.elsevier.com/computers-and-chemical-engineering`
Original file available at: `https://www.sciencedirect.com/science/article/pii/S0098135417303198`

- Compute the residuals of any specified subset of the equations at the current variable values.

- Get a sparse matrix containing the values of the partial derivatives of a specified subset of the equations with respect to a specified subset of the variables (at the object's current variable values).

The implementation of the two selected approaches, black box optimization and optimization accessing the ESO, can be graphically represented by Figures 2 and 3 respectively. The interface constructed in both cases (middleware and wrapping protocol) can be described as the result of two sub-interfaces: (i) a control interface (dash line), and (ii) an information interface (dotted line). A more detailed discussion on some specific aspects that were considered to establish these interfaces are split in the following four parts: (i) simulation, (ii) control interface, (iii) information interface, and (iv) optimization.

Simulation: Here the appropriate strategy of solution should be established, i.e., *sequential modular* or *equation oriented*. While for black box optimization it is possible to run the simulation in any mode, for the optimization accessing the ESO it is restricted to *equation oriented*.

Control interface: As a common feature for both approaches the *ActiveX* framework is used to construct the control interface, it enables communication within applications running on Windows.

Information interface: This is intended to transfer the required data. Therefore, it follows different schemes for the two distinct optimization approaches, due to the nature of the information to be transferred. The information interface for the black box optimization approach uses additional features of the ActiveX interface. Numerical values of a given set of variables (dependent and independent variables) are transferred. As explained before, since Aspen Plus does not supports the ESO CAPE-OPEN standard, an alternative approach is followed exploiting the Open Object Model Framework (OOMF). A detailed description of the script language used by the OOMF kernel is given in Aspen (2011). The middleware in this case is defined as a set of ASCII and text files that contain the required data. These are sucesively accessed to take the information either by Aspen Plus or Matlab, in

Journal homepage: https://www.journals.elsevier.com/computers-and-chemical-engineering
Original file available at: https://www.sciencedirect.com/science/article/pii/S0098135417303198

each direction. The structure given to the middleware consist of three main files. The first one contains variables information, i.e., variable name, values, scale factor, specification, and units. The second file, corresponds to the equations' information including the residual values. Finally, the last file is created to report the Jacobian. Hence all this information is generated every time the simulation converges and serves to provide the optimization routine in Matlab with the required elements at each NLP solver iteration.

Due to its dependence on creating ASCII and text files, the middleware is considered as a bottleneck for the computational performance of the proposed approach. However, it is at the authors' current best knowledge the only way provided by the OOMF to retrieve the gradient information available in the equation oriented engine of Aspen Plus. Later, the case studies show that the possible restriction imposed by this feature is compensated by the higher performance and accuracy obtained since analytically derived gradient information is being retrieved. This overcomes the main limitation of previous gradient-based approaches which depend on the numerical estimation of the gradient information through finite differences (Diaz and Bandoni, 1996; Navarro-Amoros et al., 2014). Nocedal and Stephen (1999) report that the finite differences aproximation requires n (*forward-difference*) or $2n$ (*central-difference*) more evaluations of the objective/constraint functions than the analytic differentiation, to evaluate the Jacobian. With n being the number independent variables.

In Matlab, the wrapper function interprets the information collected from the files according to Equation 2. The assumption $\mathbf{R} \approx \mathbf{0}$ is taken based on the fact that the EO engine in Aspen Plus internally solves the system of model equations by finding the values of the dependent variables $\mathbf{x}$ that minimize the residual (Apen, 2005). For this the EO engine utilizes analytical first order derivatives of the model equations and a numerical perturbation method in cases the analytical differentiation is not possible. Therefore, this guarantees the availability of the required gradient information while the residual values ($\mathbf{R}$) correspond to the error after convergence of the system of equations. These can later be used to evaluate the validity of

Journal homepage: `https://www.journals.elsevier.com/computers-and-chemical-engineering`
Original file available at: `https://www.sciencedirect.com/science/article/pii/S0098135417303198`

the results reported by the simulation. However, it should be considered that the assumption $\mathbf{R} \approx \mathbf{0}$ introduces "noise" to the NLP solver because the states and therefore the Jacobian values are not exact.

$$\begin{bmatrix} f_1(\mathbf{x},\mathbf{u}) \\ f_2(\mathbf{x},\mathbf{u}) \\ \vdots \end{bmatrix} = \begin{bmatrix} R_1 \\ R_2 \\ \vdots \end{bmatrix} \approx \mathbf{0}$$
$$\text{Jacobian} = \frac{\partial \mathbf{f}}{\partial \mathbf{y}} = \begin{bmatrix} \frac{\partial f_1}{\partial y_1} & \cdots & \frac{\partial f_1}{\partial y_{n_y}} \\ \vdots & \ddots & \vdots \\ \frac{\partial f_{n_e}}{\partial y_1} & \cdots & \frac{\partial f_{n_e}}{\partial y_{n_y}} \end{bmatrix} \tag{2}$$

Optimization: The routine for the black box optimization approach is based on NSGA-II. The MOO approach accessing the ESO is performed based on the NBI and NNC scalarization methods. For these methods the NLP solver has to be provided with the corresponding gradient information of the model at each iteration. Therefore a *Callback* structure for functions is implemented. This is a method in IPOPT for defining routines that should be executed at each iteration. Internally the *Callback* function is formulated to communicate the values of the controls, generated at each iteration of the NLP solver to the Aspen simulation via the information interface. Then the Aspen simulation runs to generate new results, which are gathered back to the *Callback* function in Matlab via the second part of the information interface. At this point the collected information is transformed into elements that can be handled by the IPOPT method. As a gradient-based NLP solver, IPOPT depends on the evaluation of the gradient of the objective and constraint functions with respect to the controls. Since the gradient information received from the information interface is the Jacobian in the form given by Equation (2), it is split into two matrices, one containing the partial derivatives with respect to the controls while the other contains the partial derivatives with respect to the states. Afterwards, the sensitivity matrix (Ascher and Petzold, 1998) (i.e., the inverse of the partial derivatives with respect to states) is operated according to Equation 3 to get the partial derivatives of the states with respect to the control variables, which in turn are required by IPOPT to fully establish the gradient of the objective and constraint functions according to Equation 4.

Journal homepage: `https://www.journals.elsevier.com/computers-and-chemical-engineering`
Original file available at: `https://www.sciencedirect.com/science/article/pii/S0098135417303198`

$$\frac{\partial \mathbf{x}}{\partial \mathbf{u}} = \begin{bmatrix} \frac{\partial x_1}{\partial u_1} & \cdots & \frac{\partial x_1}{\partial u_{n_u}} \\ \vdots & \ddots & \vdots \\ \frac{\partial x_{n_y-n_u}}{\partial u_1} & \cdots & \frac{\partial x_{n_y-n_u}}{\partial u_{n_u}} \end{bmatrix}$$

$$\frac{\partial \mathbf{x}}{\partial \mathbf{u}} = \begin{bmatrix} \frac{\partial f_1}{\partial x_1} & \cdots & \frac{\partial f_1}{\partial x_{n_y-n_u}} \\ \vdots & \ddots & \vdots \\ \frac{\partial f_e}{\partial x_1} & \cdots & \frac{\partial f_e}{\partial x_{n_y-n_u}} \end{bmatrix}^{-1} \begin{bmatrix} \frac{\partial f_1}{\partial u_1} & \cdots & \frac{\partial f_1}{\partial u_{n_u}} \\ \vdots & \ddots & \vdots \\ \frac{\partial f_e}{\partial u_1} & \cdots & \frac{\partial f_e}{\partial u_{n_u}} \end{bmatrix} \tag{3}$$

$$\nabla_u \begin{bmatrix} \mathbf{J}(\mathbf{y}) \\ \mathbf{g}(\mathbf{y}) \end{bmatrix} = \begin{bmatrix} \nabla_u \mathbf{J}(\mathbf{u}, \mathbf{x}) \\ \nabla_u \mathbf{g}(\mathbf{u}, \mathbf{x}) \end{bmatrix} = \begin{bmatrix} \mathbf{p}(\frac{\partial \mathbf{J}}{\partial \mathbf{u}}, \frac{\partial \mathbf{J}}{\partial \mathbf{x}} \frac{\partial \mathbf{x}}{\partial \mathbf{u}}) \\ \mathbf{q}(\frac{\partial \mathbf{g}}{\partial \mathbf{u}}, \frac{\partial \mathbf{g}}{\partial \mathbf{x}} \frac{\partial \mathbf{x}}{\partial \mathbf{u}}) \end{bmatrix} \tag{4}$$

In order to make the gradient information available to IPOPT, two different approaches have been implemented:

Linearization of the states:. Linear functions were formulated in the form $\mathbf{x} \approx \frac{\partial \mathbf{x}}{\partial \mathbf{u}}\mathbf{u} + \mathbf{C}$ to represent the system of flowsheet equations in the process simulator. These are valid only locally and therefore are updated at each iteration of the IPOPT solver with the values for $\frac{\partial \mathbf{x}}{\partial \mathbf{u}}$ and $\mathbf{C}$. This is a dummy formulation that serves only to transfer the gradient information to the IPOPT routine.

Embedding a function and its Jacobian:. Alternatively a more complex programing structure involves developing functions for embedding the states as callback functions with a known Jacobian matrix ($\frac{\partial \mathbf{x}}{\partial \mathbf{u}}$) in CasADi. This approach offers the same numerical outcome as the previous one, but the differentiation of the states in Matlab is not needed during the optimization. As part of the first case study these two approaches will be compared.

The developed Interface for gradient-based MOO of processes simulated in Aspen Plus is refered as INPROP (INterface for PRocess OPtimization). The Matlab scripts that constitute this software tool are made freely available for academic purposes on the website https://cit.kuleuven.be/biotec/software/inprop-1. Complete details on the described interface can be found in these scripts. Additionally, the files corresponding to the three implemented case studies are available as well in

Journal homepage: `https://www.journals.elsevier.com/computers-and-chemical-engineering`
Original file available at: `https://www.sciencedirect.com/science/article/pii/S0098135417303198`

this website as supplementary files.

4. Case studies

In the first subsection the debutanizer column case study is presented. It is used as an illustrative case to evaluate and compare the performance and limitations of the methods implemented in the optimization interface, i.e., scalarization and vectorization methods. The butyl acetate and the methanol production processes are introduced as more complex case studies to exploit the developed optimization interface with the gradient-based scalarization approach in industrially relevant flowsheets.

4.1. Debutanizer

The deubutanizer column is is a common distillation unit in refineries, it is used as part of different processes to fractionate light products. For instance on a delayed coking unit the debutanizer column is part of the vapor recovery section where an improved separation between the gas and naphtha coming from the delayed coking unit is achieved. The implemented Aspen simulation for this process is made available as the Supplementary file A. In Figure 4 the simulated column with the independent and dependent variables is presented. The composition of the feed stream is presented in Table 1. Some approximations used in the simulation for this composition are the following: (i) the butenes are approximated by pure 1-butene, (ii) fractions defined by range of boiling points are approximated by a single compound (hydrocarbon) with a boiling point in the middle of the range. For the C_5 - 453.15 K fraction, n-heptane is being used, this alkane boils at 373.15 K. For the 453.15 K - 623.15 K fraction 1-pentadecane is used, as this alkane has a boiling point at 544.15 K.

Two commonly used equations of state for this kind of systems are: (i) Peng-Robinson (PR) and (ii) Soave-Redlich-Kwong (SRK). In Ahmadi et al. (2015) the accuracy of a set of property methods for a debutanizer column regarding actual real measurements is investigated finding that PR is the most accurate method for this system. For the simulations the *Radfrac* method in Aspen Plus is chosen

Journal homepage: `https://www.journals.elsevier.com/computers-and-chemical-engineering`
Original file available at: `https://www.sciencedirect.com/science/article/pii/S0098135417303198`

in combination with the ideal equilibrium model. The latter differs from the rate based model as it does not take into account limitations due to heat-mass transfer and liquid-vapor diffusion. Additionally, the efficiencies for all trays are set equal to one. Other specifications needed for the simulations are introduced in Table 2. For this case study the *reflux ratio* (RR) and the *distillate rate* are to be used as the independent variables or controls in the optimization. The remaining states and an overview of the control variables are given in Table 3.

4.2. Butyl acetate production

A commercially viable chemical route to produce butyl acetate is based on the transesterification of methyl acetate (MeAC) using butanol (BuOH) (Tang et al., 2005). This category of reactions corresponds to an ester reacting with an alcohol in the presence of a catalyst. From this reaction a new couple ester-alcohol is produced due to the exchange of the organic groups present in the feed. In this case study the products are butyl acetate (BuAc) and methanol (MeOH) (Luyben et al., 2004). The exact chemical reaction is presented in Equation (5). This process has been proven to be economically feasible, because the MeAC, which is a low value side product from the production of poly-(vinyl)-alcohol (PVA), is converted into MeOH and high purity BuAc. The former product is recycled as feedstock for the PVA production (Steinigeweg and Gmehling, 2004) while the BuAc can be used in many applications and has a higher added value.

$$\begin{gathered} \mathrm{CH_3COOCH_3} + \mathrm{CH_3(CH_2)_3OH} \leftrightharpoons \mathrm{CH_3COO(CH_2)_3CH_3} + \mathrm{CH_3OH} \\ \mathrm{MeAc} + \mathrm{BuOH} \leftrightarrow \mathrm{BuAc} + \mathrm{MeOH} \end{gathered} \tag{5}$$

The complete production process requires multiple separation stages to achieve high purity outlet streams and recover most of the reactants. The main difficulty in this separation is the presence of two binary azeotropes in the mixture: (i) methyl acetate and methanol and (ii) butyl acetate and butanol (Luyben, 2011). Therefore multiple production approaches have been proposed. The traditional approach consist of a *Continuous Stirred Tank Reactor* (CSTR) followed by a set of separation columns, for which two techniques are commonly used: i.e., pressure swing distillation and the use of an entrainer (Jimenez et al., 2002). Several alternatives

Journal homepage: https://www.journals.elsevier.com/computers-and-chemical-engineering
Original file available at: https://www.sciencedirect.com/science/article/pii/S0098135417303198

to the traditional process have been investigated. Gangadwala and Kienle (2007) evaluates an option based on a reactive distillation column and side reactor coupled with non-reactive distillation columns. However, this case study is based on the traditional scheme using the pressure swing technique for the separation stage.

In Figure 5 the simulation flowsheet of the butyl acetate production process is presented. This corresponds to the simulation developed by Verheyden (2014) which in turn is based on the flow diagram and operation conditions for the process presented by Luyben et al. (2004). These operational conditions are used in this work as a benchmark to check the achieved improvements via process optimization. In the process the input streams consisting of MeAc and BuOH are brought into a CSTR at the given conditions. Inside the reactor the transesterification reaction takes place, as a reversible reaction, catalyzed by a strong acid (Wang et al., 2008). The reaction kinetics are given according to Equation 6. Some thermodynamic properties of this reaction are: (i) the equilibrium constant is close to the unit, therefore the dependence on the temperature is weak and (ii) the enthalpy of the reaction is low (Luyben et al., 2004). The outlet stream from the reactor, containing the four involved chemical substances is then sent to the first distillation column. From this the top product is rich in MeAc and MeOH while the bottom product is a mixture of mainly BuAc and BuOH. For the light product a second separation step is applied, in this case the top product is a mixture at almost the azeotropic MeAc-MeOH composition. This stream is recycled to the reactor. The bottom product of the second distillation column is almost pure methanol. Meanwhile the heavy product from the first distillation column is also subsequently separated, in this case into high purity BuAc as bottom product and a stream concentrated on BuOH, which is recycled to the reactor (Luyben et al., 2004).

$$\begin{aligned} r &= k_F C_{MeAc} C_{BuOH} - k_R C_{BuAc} C_{MeOH} \\ K_F &= 7 \cdot 10^6 e^{-71960/RT} \\ K_R &= 9.467 \cdot 10^6 \exp^{-72670/RT} \end{aligned} \tag{6}$$

Due to the complexity of the mixtures, for which two binary azeotropes occur, an activity model is required to describe the vapor-liquid equilibrium present in the

Journal homepage: https://www.journals.elsevier.com/computers-and-chemical-engineering
Original file available at: https://www.sciencedirect.com/science/article/pii/S0098135417303198

system. For this (Verheyden, 2014) uses NRTL in the simulation. Table 4 contains a summary of the fixed process conditions and parameters to model the butyl acetate production process, the detailed information can be found in the Supplementary file B. Table 5 presents the complete list of variables and states used to formulate the MOO problem.

4.3. Methanol production via methane tri-reforming

Traditionally one of the more common commercial routes to produce methanol is the catalytic conversion of syngas (gas mixture of carbon monoxide CO and hydrogen H_2). There exist many carbon sources that can be used as feedstock to obtain syngas. An increasing attention goes to production routes exploiting the valorization of side streams, renewable materials and waste, since value is added to these material streams with an environmentally positive impact. Recently particular attention has been focused to the methane tri-reforming, as an alternative approach for the conversion of CO_2 in the flue stack gas without the CO_2 pre-separation (Song and Pan, 2004). Thus producing methanol from methane and flue gas involves two reaction stages. First the tri-reforming, which is a complex thermo-chemical conversion involving several reactions to convert CH_4, CO_2, O_2 and H_2O into syngas. Zhang et al. (2013) present the set of 9 reactions normally related to this conversion. Secondly, for the methanol production, the syngas in a proportion H_2/CO around 2 is brought to reaction conditions to produce a mixture of MeOH and water. In Equation (7) the methanol production reactions are presented. The third reaction corresponds to the reversible water gas shift reaction (Navarro-Amoros et al., 2014).

$$\mathrm{CO} + 2\mathrm{H_2} \rightarrow \mathrm{CH_3OH} \tag{7a}$$

$$\mathrm{CO_2} + 3\mathrm{H_2} \rightarrow \mathrm{CH_3OH} + \mathrm{H_2O} \tag{7b}$$

$$\mathrm{CO} + \mathrm{H_2O} \leftrightarrow \mathrm{CO_2} + \mathrm{H_2} \tag{7c}$$

Figure 6 corresponds to the flowsheet modeled in Aspen Plus for this case study. This is the production scheme proposed and studied by Zhang et al. (2013). In the process, the two gas streams (flue gas and methane) are put together and preheated

Journal homepage: https://www.journals.elsevier.com/computers-and-chemical-engineering
Original file available at: https://www.sciencedirect.com/science/article/pii/S0098135417303198

to the reaction temperature before entering into the reactor. The tri-reforming is modeled in a Gibbs reactor which computes the composition at the outlet as the equilibrium composition, that minimizes the total Gibbs free energy over all the species, at the reactor conditions. The reactor output is then cooled down and compressed. After achieving the desired reaction pressure for the methanol production, the temperature is adjusted, cooling or heating is required depending on the desired reaction temperature. As suggested by Zhang et al. (2013) the methanol reactor is modeled as an equilibrium reactor considering only reactions (7a) and (7b), since in these conditions the the water gas shift reaction is linearly dependent and its conversion is negligible. As part of preliminary studies the CO and CO_2 conversion of the modeled methanol reactor were validated with respect to the values reported by Navarro-Amoros et al. (2014). This validation showed adequate results in the range between 5 to 30 MPa and from 480 to 570 K. After reaction, the gaseous product is expanded and cooled down to separate most of the methanol and water from non-condensable gases. The gas separated in the flash drum contains high levels of unreacted syngas due to the low conversion in the methanol reactor. Therefore this stream is recirculated to the reactor. A purge is taken from the recycle stream to avoid accumulation of inert gases (mainly N_2) in the loop. The recycle stream has to be compressed to enter the reactor again. The liquid product from the flash separation is then expanded again to reduce even further the amount of non-condensable gases and then the remaining liquid is distilled to adjust the quality of the methanol product to be $\geq$99,5%.

As suggested by Zhang et al. (2013), Peng Robinson equation of state was the thermodynamic model implemented for this flowsheet simulation. The optimal conditions reported by Zhang et al. (2013) were reproduced to serve as reference and to evaluate the advantages of the results obtained via MOO of the process. Following the same approach presented by Navarro-Amoros et al. (2014) the kinetics of the methanol reactions were considered only to determine the reactor volume required to achieve the equilibrium concentrations predicted in Aspen Plus. The reader can find the kinetic models and parameters in Navarro-Amoros et al. (2014). Table 6 contains a summary of fixed process conditions and parameters to model

Journal homepage: https://www.journals.elsevier.com/computers-and-chemical-engineering
Original file available at: https://www.sciencedirect.com/science/article/pii/S0098135417303198

the methanol production process, the detailed information can be found in the Supplementary file C. The independent variables were selected based on what previous studies have evaluated about this process (Zhang et al. (2013); Navarro-Amoros et al. (2014); Luyben (2010)), and what are considered to be the most important operational parameters for this process. Table 7 presents the complete list of independent variables and states involved in the formulation of the MOO problem.

5. Simulation results

Section 5.1 discusses the results for the debutanizer while the results for the butyl acetate and methanol production processes are presented in sections 5.2 and 5.3 respectively.

5.1. Debutanizer

As this case study serves to illustrate and compare the results obtained by applying the two possible MOO approaches, two different MOO optimization formulations are evaluated. The first problem is based on objective J_1, which has no physical interpretation but was chosen to highlight the advantages and main issues of each approach. This function was formulated to exhibit two optimal solutions in the feasible space, and it is given according to:

$$\begin{aligned} J_1 = &- \left(p_1 u_2 \frac{1}{p_2 x_3^2} + p_3 x_4 - p_4 x_1^2 - p_5 x_2 - p_6 x_3 - e^{p_3 u_1 u_2}\right) \\ & p_1 = 2.266 \cdot 10^{-3} \qquad p_2 = 185.185 \\ & p_3 = 7.854 \cdot 10^{-4} \qquad p_4 = 1.712 \cdot 10^{-5} \\ & p_5 = -1.626 \cdot 10^{-5} \quad p_6 = 555.555 \end{aligned} \tag{8}$$

In contrast the second MOO problem is based on a realistic profit function for the debutanizer column (J_2). This is based on the formulation and the values presented by White (2012). This function considers the income as result of the price for both products which are affected by the quality. Different from the case evaluated in the reference, in this case a step increase in the price for the top product is applied through a logistic function, while a linear increase on the price is formulated for the bottom product. The costs correspond to the energy consumption and the raw material. The total is expressed in relative terms, based on the mass inlet flow.

Journal homepage: https://www.journals.elsevier.com/computers-and-chemical-engineering
Original file available at: https://www.sciencedirect.com/science/article/pii/S0098135417303198

This function is formulated in Equation 9. The logistic function that determines the price for the distillate product is defined to establish two conditions, a low quality product ($> 4\%\ C_5$) and a high quality product ($< 4\%\ C_5$).

$$\begin{aligned} J_2 =& -(\text{income} - \text{costs})/x_8 \quad [\$/\text{kg}] \\ \text{income} =& u_2 \left(\frac{a_1}{1 + e^{(-a_2(x_3 - a_3))}} + a_4 \right) + x_4(a_5(x_5 + x_6 + x_7 - a_6) + a_7) \\ \text{costs} =& a_8 x_7 + a_9(x_1 + a_{10} x_2) \\ & a_1 = 0.240 \qquad a_4 = 0.480 \qquad a_7 = 0.740 \qquad a_{10} = 0.500 \\ & a_2 = -500 \qquad a_5 = 8.0 \qquad a_8 = 0.740 \\ & a_3 = 0.040 \qquad a_6 = 0.017 \qquad a_9 = 0.0140 \end{aligned} \tag{9}$$

Two additional objective functions are specified to complete the two MOO formulations. The aim is to investigate conflicting objectives that are normally considered as accounted by the profit function. Constructing the Pareto front for this problem allows a sensitivity analysis on the tradeoffs between the different objectives to enhance process understanding and to made a more thorough decision on the chosen optimal operational conditions. These functions are the total energy consumption J_3 and the quality of the distillate product J_4. The former is defined as the sum of the condenser and reboiler duties, while the quality of the distillate product is established by the content of n-Pentane (nC_5) in the stream. Equation 10 denotes objective functions J_3 and J_4. The constraints for this problem are the minimum quality for the bottom product and the controls boundaries, given in Equation 11.

$$\begin{aligned} J_3 &= \sum_{i=1}^{2} |x_i| \quad [MW] \\ J_4 &= x_3 \qquad [wt.frac.] \end{aligned} \tag{10}$$

$$\begin{aligned} & g(x) : x_5 - 0.01 \leqslant 0 \\ & 5 < u_1 < 25 \\ & 9000 < u_2 < 25000 \end{aligned} \tag{11}$$

Journal homepage: https://www.journals.elsevier.com/computers-and-chemical-engineering
Original file available at: https://www.sciencedirect.com/science/article/pii/S0098135417303198

5.1.1. Single objective optimization

Here only the illustrative objective function is considered in order to evaluate and compare performance aspects of the methods applied. In Figures 7 and 8 the obtained results are presented. These denote contour graphs where the axes correspond to the control variables, distillate rate (u_2) against reflux ratio (u_1), and the colored contour lines correspond to different value levels for the objective function. On these graphs the black dashed line represents the quality constraint ($g(\mathbf{x})$) when it is exactly equal to zero, which along with the contour lines were drawn from a sensitivity analysis. In the figures the red points correspond to the results at each iteration of the NLP solver while the blue marks are the (local) optimal points in each case. Two cases are presented for each approach. In the case of the optimization accessing the ESO (Figures 7a and 7b), the difference is the convergence to two distinct optimum solutions. Since the direction of convergence is determined by the initial guesses for the controls, the effect of two different initial values can be seen in the figures. For the case in Figure 7a the best known minimum is found with the initial guess $\mathbf{u}_0$ as $[20, 11000]$ while for Figure 7b the local minimum is obtained for $\mathbf{u}_0$ is $[20, 11500]$. This shows the need for applying globalization procedures like the multiple starting point search when using gradient based methods.

The black box optimization results for different parameter values of the *gamultiobj* function, are presented in Figures 8a and 8b. The former corresponds to the case when the problem is solved with the default values, the problem does not converge to a solution and remains iterating in the neighborhood of the optimal solution. Figure 8a is the result if the iteration is forced to stop. In addition to the no convergence problem, a limited accuracy for satisfying the imposed constraint is observed. As can be seen in Figure 8 most of the results are in the neighborhood of the constraint line however only a few of them are exactly on the line or above it which are the conditions for fulfilling the constraint $g(x) \leq 0$. This means that at least under the default parameters, the genetic algorithm has limitations for convergence and satisfaction of the inequality constraint. In order to overcome these limitations the effect of modifying some parameters has been investigated. Population size, function tolerance and maximum stall generations have been adapted. In general

Journal homepage: https://www.journals.elsevier.com/computers-and-chemical-engineering
Original file available at: https://www.sciencedirect.com/science/article/pii/S0098135417303198

the successful strategy has been to reduce population size, imposing milder stopping criteria and offering lower tolerance to validate constraint satisfaction. One of the closest solutions obtained from this evaluation is presented in Figure 8b. The chosen parameters to produce this solution are: population size = 10, function tolerance $= 1 \cdot 10^{-4}$, maximum stall generations = 30 and constraint tolerance $= 5 \cdot 10^{-4}$. A clear improvement is observed regarding the constraint satisfaction, however the result obtained is far from the optimal solution.

In Table 9 the numerical results are presented. Only the results for the cases where the best known optimum is obtained are reported. In the case of black box optimization the reported values corresponds to the solution presented in Figure 8b. Regarding the optimization accessing the ESO two sets of results are presented. These correspond to using the two methods implemented for transferring the gradient information to IPOPT. As it can be seen the difference on the results is not significant, being lower than 0.1% for the objective function. In terms of computational time, as expected the time required by the gradient-based approach is lower than the black box optimization, this should correspond with fewer evaluations required of the objective function and therefore lower time spent on the solution of the flowsheet simulation.

5.1.2. Multiobjective optimization

First, the bi-objective problem, using the illustrative function and the total energy demand (J_1 and J_3), is solved. The results for the optimization accessing the ESO, and the black box optimization are depicted in Figure 9. In both cases the optimization problem was solved defining a feasible space that guarantees the presence of the two known optimal solutions on the illustrative function. For the convergence of the black box optimization the quality constraint was imposed as design specification in the simulation. This guarantees fulfilling the constraint condition while simplifies the optimization problem so the NSGA-II method has to solve a constraint-free problem. Thus the limitation of the genetic algorithm to cope with constraints is surpassed, however this impose an extra limitation because the design specifications in Aspen Plus can be only equality conditions. In Aspen Plus a design specification is an additional equation that has to be solve in the

Journal homepage: `https://www.journals.elsevier.com/computers-and-chemical-engineering`
Original file available at: `https://www.sciencedirect.com/science/article/pii/S0098135417303198`

system. Additionally, some parameters of the *gamultiobj* function are adjusted different from the default values. This is the function tolerance $= 1 \cdot 10^{-2}$, maximum stall generations = 10, and Pareto fraction = 0.3. The last parameter is used to control the elitism of the genetic algorithm and in this case is adjusted to generate a Pareto front with the same number of points produced by the ESO approach, so the results are comparable.

In Figure 9 the results from both methods for the Pareto front are plotted together with the curve that describes the border of the feasible space for the problem. This is obtained via sensitivity analysis and contains exact solutions. From these results some aspects are highlighted. First, a high accuracy is observed on the results from both optimization methods, but with limited reproducibility of the Pareto front. In the case of the ESO approach non-optimal Pareto solutions are present, while for the black box optimization the optimal points do not represent a uniform spread over the Parteo front. The non-optimal Pareto solutions are solutions at the border of the feasible region, that are dominated by other point in the Pareto front. When this is verified, it can be observed that only the Pareto front obtained via black box optimization meets the condition for all its points. The Pareto front obtained from the ESO approach contains a sub-set of 4 solutions which are non-optimal Pareto points, because there are other solutions that for the same values of J_1 require lower energy J_3 . Therefore, the solution for this bi-objective problem is a discontinuous Pareto front due to the presence of two minimun points for one of the objective functions. Regarding the computational cost, Table 10 presents the time required for convergence in each case. The fastest performance is obtained again for the gradient-based approach.

Finally the MOO with three objectives is formulated, i.e., illustrative function J_1, total energy demanded J_3 and distillate quality J_4 are considered. In this case the feasible space is defined to be only in the region of the best known minimum for the illustrative function which is the desired result. In Figure 10 the solutions generated by black box optimization and accessing the ESO are depicted. The black box optimization approach produces a solution that is restricted to a line, this is presented

Journal homepage: https://www.journals.elsevier.com/computers-and-chemical-engineering
Original file available at: https://www.sciencedirect.com/science/article/pii/S0098135417303198

in the Figure with small circles(o). It is interesting to see how this solution links the three anchor points, however it is only a subset of the Pareto points generated by the ESO approach.

To efficiently solve MOO problems via ESO approach some adjustment on the options for the IPOPT solver can be applied. This to guarantee convergence of the solver and increase computational performance using milder termination conditions. In Table 12, the used solver parameters are reported for the three case studies. Finally, the performance of the two optimization approaches is illustrated in Table 10. These correspond to the solutions depicted in Figure 10. The high efficiency of the black box optimization should be noted. However, it should be considered that in this case the result is limited to just one part of the Pareto front generated via the ESO approach. Therefore it offers a very limited amount of information. A similar behavior has been discussed by Logist et al. (2013). Note that in general for all results the performance of the gradient-based approach performs worse with the embedded function than with the simple states linearization.

In contrast with the previous results, that serve only to evaluate the performance of the methods, the MOO problem formulated based on the profit function J_2, the energy consumption J_3 and the distillate quality J_4 serves to critically evaluate optimal operational conditions for the debutanizer column. The results via ESO and black box approach corresponding to this MOO problem are presented in Figure 11. In this case it was decided to impose the problem's inequality constraint explicitly in the optimization problem formulation for the black box approach. Thus both approaches are implemented in the same way in order to be compared. As expected since no design specification are set in Aspen Plus, the black box optimization produces a set of Pareto solutions (black circles (o)) that is spread over the Pareto front. However the solution via the ESO approach remains more informative because of the even distribution of the Pareto points. Additionally, many of the optimal solutions obtained via black box optimization are out of the region between individual minima, some of the solutions present small violations of the quality constraint and the three anchor points are not part of the solution. Re-

Journal homepage: https://www.journals.elsevier.com/computers-and-chemical-engineering
Original file available at: https://www.sciencedirect.com/science/article/pii/S0098135417303198

garding computational performance, the results presented in Figure 11 comprise 45 points in both cases and its convergence required 2.61 and 2.65 minutes for ESO and black box approach respectively. In this case both optimization approaches offer equivalent computational performance, therefore the ESO approach should be preferred because of the better quality of the results.

From the results in Figure 11 the conflictive character of the three objectives is clear. Even though the profit function (Equation 9) depends on both terms, i.e., distillate quality and energy consumption, the behavior of none of them is fully correlated to the profit function. From these results it is interesting to see how the maximum profit results from having a low quality distillate($> 4\%$ C_5), these can be attributed to the fact that for those conditions higher quality is achieved for the bottom product, which influences the profit function more because of its linear increase on price and the higher productivity. Additionally, this result is achieved at a lower energy demand than if high quality were desired for both top and bottom products. In terms of sensitivity analysis or the opportunity cost the Pareto front presents what would be interesting regions for a decision maker. The region of optimal solutions close to the maximum profit shows how lowering the profit on small proportions can generate significant reductions on energy demand and improvements on the quality of the product. An interesting tradeoff for the decision maker would be to evaluate the solutions with a high quality distillate($< 4\%$ C_5) to see how the profit and energy demand are affected. This is for instance a distillate with 3.9 % C_5 can be obtained with 11.4 MW less energy demanded and only a reduction of 4.2 % in the profit for the operation. The later profit reduction is due to the reduction on the quality of the bottom product. An alternative approach to reflect the value of the information provided on the Pareto front is the ease on evaluating the opportunity cost for certain decisions, e.g., if the energy provided to the process is reduced or limited the impact can be rapidly determined and new operational conditions established to guarantee the best possible outcome.

5.2. Butyl acetate production

Two different MOO problems were evaluated for this case study. As common objective functions, the total energy demanded (J_1) and the recycle flow (J_2) in the

process were minimized. The benefit obtained by any improvement in the former objective is clear while for the latter, an indirect improvement of the process is expected. The reduction of inventories circulating in the process, which directly implies the reduction in size of equipments, pipelines and accessories (e.g., valves and fittings) is one of these positive effects. The first MOO optimization problem is completed with the quality of the methanol produced as by-product as third objective function (J_3). For the original process a benchmark of purity $> 92.8\%$ is specified. This quality specification is traditionally sufficient since the product is recycled to the PVA production. However, the tradeoff between a higher quality of this product and the energy demand might result in a more valuable outcome. The second MOO problem formulated for this case study replaces the quality objective function by a profit-cost function (J_4). As in the first case study including this objective results in a more realistic application of the proposed interface on a practical-industrially relevant case.

The first objective function corresponding to energy consumption is given in Equation (12a). The total recycle flow is expressed as the summation of the two distillate streams from columns C2 and C3 which are totally recycled in the process. Equation (12b) denotes this objective function. For the quality of the methanol product stream the formulation is given in Equation (12c), and it corresponds to the maximization of the molar fraction of methanol in the product stream from column C2. Finally the profit-cost function is presented in Equation (13). To determine the profit over the process operation, the sales of the two products i.e., butyl acetate and methanol are considered as income. A fixed price is considered for the butyl acetate, since it is accepted only at the quality standards. In contrast methanol has only a lower quality bound and a higher purity is technically feasible. Therefore the value of any improvement in the methanol quality is weighted through a price function. Similar to the profit function for the debutanizer, a logistic function was used to establish price levels depending on the product quality. In this case the methanol was evaluated at three different quality conditions, a low quality product ($> 92.8\%\ CH_3OH$), a medium quality ($> 98.5\%\ CH_3OH$) and a high quality product ($> 99.5\%\ CH_3OH$). The operational costs result from the needed energy

Journal homepage: https://www.journals.elsevier.com/computers-and-chemical-engineering
Original file available at: https://www.sciencedirect.com/science/article/pii/S0098135417303198

and the feedstock. Value is only assigned to the butanol stream, because as explained before the input stream containing methyl acetate is a side stream from the PVA process. In Equation (14) the mathematical formulation of the complete optimization problem is presented.

$$J_1 = \sum_{i=1}^{15} |x_i| \quad [MW] \tag{12a}$$

$$J_2 = x_{18} + x_{19} \quad [kmol/s] \tag{12b}$$

$$J_3 = -x_{16} \quad [mole.frac.] \tag{12c}$$

$$\begin{aligned} J_4 &= -\left(\text{income} - \text{costs}\right) \quad [\$/h] \\ \text{income} &= a_1 x_{21} + \left(\frac{a_2}{1 + e^{(-a_3(x_{16} - a_4))}} + \frac{a_5}{1 + e^{(-a_6(x_{16} - a_7))}} + a_8 \right) x_{20} \\ \text{costs} &= a_9 x_{22} + 3600 \times a_{10}(-x_2 - x_3 - x_6 - x_{11} - x_{13}) + \\ &\quad 3600 \times a_{11}(x_8 + x_{14} + x_{15}) + a_{11}(x_1 + x_4 + x_5 + x_7 + x_9 + x_{10} + x_{12}) \\ &\quad a_1 = 0.9000 \qquad a_4 = 0.9935 \qquad a_7 = 0.9790 \qquad a_{10} = 1.0 \times 10^{-10} \\ &\quad a_2 = 0.30 \qquad a_5 = 0.20 \qquad a_8 = 0.20 \qquad a_{11} = 9.0 \times 10^{-5} \\ &\quad a_3 = 6000 \qquad a_6 = 600 \qquad a_9 = 0.60 \qquad a_{12} = 8.98 \times 10^{-9} \end{aligned} \tag{13}$$

$$\begin{aligned} &\min_{\mathbf{u} \in R^6} \quad [J_1,\, J_2,\, J_3] \\ \text{s.t.:} \quad &g_1(x) : 0.928 - x_{16} \leqslant 0 \\ &g_2(x) : 0.995 - x_{17} \leqslant 0 \\ &0.24 < u_1 < 0.4 \qquad 0.55 < u_2 < 0.62 \\ &0.75 < u_3 < 1.2 \qquad 0.5 < u_4 < 0.7 \\ &1.87 < u_5 < 2.5 \qquad 0.65 < u_6 < 0.75 \end{aligned} \tag{14}$$

In Figure 12 the optimal results are depicted for both optimization problems. Figure 12a corresponds to the methanol quality-based Pareto front, while Figure 12b presents the results for the profit-based MOO optimization. In both cases the solution is presented with reference to the original process conditions (+). From Figure 12 the optimization potential of the process becomes clear. Hence, these

Journal homepage: https://www.journals.elsevier.com/computers-and-chemical-engineering
Original file available at: https://www.sciencedirect.com/science/article/pii/S0098135417303198

results can be studied to evaluate the advantages that each individual optimal condition offers and the possible tradeoffs between them. The optimal solutions for the four objectives are presented in Table 11, together with the reference condition of the original process (Luyben, 2011). The optimal solution for the energy demand (J_1) results in a reduction of 2.214 [MW] which is a reduction of 9.94%. If the the recycle flows are minimized (J_2), a total reduction of 0.0239 [kmol/s] is achieved, this is equivalent to 29.2% less than the original total recycle flow. From these individual minima it is interesting to see that contrary to what can be expected, having the maximum reflux ratio in the columns does not necessary imply the highest total energy demand. This is explained by the fact that by increasing the reflux ratio, a higher purity is obtained on the top products which in turn are recycled to the reactor section with lower contents of the product substances. This means shifting the reaction equilibrium towards the products which in turn drives to higher conversion and then at the end less material have to be processed by the distillation train. For this specific result, the energy demand is even lower than in the original process (21.419 vs. 22.284 [MW]). Furthermore, the corresponding distillate to feed ratios in each column can be seen as the adjusted variable to meet the quality constraints.

In the case of maximizing the methanol quality (J_3) the molar concentration of methanol in the product stream (bottom of the C2-column) increases from the benchmark value, 92.8% to 99.6%. This improvement brings the product quality closer to the commercial grade for methanol. To achieve this optimal condition, the controls are varied to a new condition that favors the purification of methanol. As it can be seen in Table 11, it is the optimal condition with the highest distillate to feed ratio (u_4) and a relatively low reflux ratio (u_3) in column C_2. This explains the high purity on the bottom stream (methanol), but it also implies larger flow and lower quality for the distillate, which goes against the conditions identified for low energy demand. In fact, this optimal condition implies the highest total energy demand and total recycle flow from the possible solutions. Finally the conditions for maximum profit (J_4) are similar to those achieved for maximum methanol quality. However, the methanol quality is slightly lower, being sufficient to achieve the maximum value of the logistic price function. The consumed energy is significantly

Journal homepage: https://www.journals.elsevier.com/computers-and-chemical-engineering
Original file available at: https://www.sciencedirect.com/science/article/pii/S0098135417303198

less not only due to the reduction of the methanol quality but because of the explicit inclusion of the energy cost in the objective function. The optimal solution for the profit function is in fact a specific tradeoff point between quality and energy. This can be seen when comparing the two Pareto fronts in Figure 12. The individual maximum for the profit function corresponds to a Pareto point in the valley region close to the optimal methanol quality in Figure 12a. The optimal values for the independent variables show that one of the reasons for maximum profit is a lower distillate to feed ratio (u_4) in column C_2 than for the optimal quality, being this a reason as well for the lower energy demand compare to the maximum methanol quality.

Regarding different tradeoff solutions for the butyl acetate process, in Figure 12 the obtained Pareto fronts present steep regions between, on the one hand, the energy and recycle anchor points and on the other hand, the quality of methanol or the profit. In case of Figure 12a, it is only after high quality values are reached (mole fraction>0.985) that a pronounced change on direction is seen, making any further increase on quality highly expensive in terms of energy demand, with a fast increase on the required recycle and therefore with a less significant gain on the profit. This can be considered as a favorable property in case the desired tradeoff between these objectives is to have a significant increase in methanol purity and therefore profit but keeping energy demand and recycle flow below the original process values. One possible solution corresponds to the optimal solution having 99.4mole% of methanol purity and the minimum energy demand. Thus for this solution the energy demand would be 21.1925 [MW] and the recycle flow 0.066 [kmol/s]. This solution represents a tradeoff where 97% of the potential improvement on quality is achieved while 49% and 66% of their potentials reductions are achieved for energy demand and recycle flow. The maximum potential of improvement for each objective function corresponds to pass from the original process condition to each individual optimal solution. Other optimal solutions can be chosen depending on the decision maker's preferences or criteria. From Figure 12b it is interesting to see that this Pareto front has a combination of concave and convex regions, which are attributed manly to the steps on the price function for methanol. Additionally the region towards

Journal homepage: https://www.journals.elsevier.com/computers-and-chemical-engineering
Original file available at: https://www.sciencedirect.com/science/article/pii/S0098135417303198

the border of minimum energy in the Pareto front shows a very particular behavior. Since the improvement on methanol quality is restricted due to the condition of low energy demand, the profit is kept relatively low till the point when the limitation is overcome and a very sharp increase in profit is produce due to the sudden increase in methanol quality.

Regarding convergence of the series of parametric SOOPs (the tradeoff points of interest) issues occurred when the NBI method was applied. It is considered that the noise introduced by the convergence error tolerance in Aspen Plus affects the solution of the parametric subproblems more than the original single objective problems, this convergence issue is discussed as well by Jang et al. (2005). Therefore, since the NBI method transforms the three objective functions into equality constraints to formulate the parametric single objectives, the problem becomes more complex and sensitive to be affected by noise. Hence the NNC method is used as alternative. Since this method is based on the same principle applied by the ε-constraint method, the resulting parametric formulation does not depend on modifying and combining the objective functions and therefore is assumed to be less prone to the same issues experienced with NBI.

In order to prevent or reduce the possible negative effect of noise propagation from the inexact convergence of Aspen Plus to the NLP solver some aspects can be considered when modeling the process, formulating and solving the NLP problem. The equation oriented mode of Aspen Plus offers several parameters to configure its internal NLP solver, e.g., method applied, tolerances, number of iterations. These features can be adjusted to reduce as much as possible the residual value after convergence ($\mathbf{R}$) and therefore to have more accurate solutions for the states and Jacobian. However imposing tight conditions (e.g., very low tolerances) can turn the model unstable reducing convergence robustness and making the optimization parsimonious. In case the process model contains non supported units for analytical derivation in the EO mode, the perturbation size for the numerical derivation that is applied in Aspen Plus, can be adjusted to find and equilibrium between error in the approximation and convergence noise. Navarro-Amoros et al. (2014) discusses

Journal homepage: https://www.journals.elsevier.com/computers-and-chemical-engineering
Original file available at: https://www.sciencedirect.com/science/article/pii/S0098135417303198

how to reduce the noise amplification due to recycles in the flowsheet. The system can be modeled with open recycles so the simulator does not have to converge for those streams. This task is transferred to the external NLP solver. Even though the optimization problem becomes larger (i.e., more variables and explicit equality constraints) the use of the explicit solver makes the solution more robust, less prone to noise and the computational time was found to be similar. Finally, as observed in this contribution for MOO the NNC method should be preferred over the NBI. In general, methods that do not require adding explicit nonlinear equality constraints should be preferred.

Through preliminary evaluations it was found that higher convergence robustness can be given to the model in Aspen Plus if additional constraints are set to the optimization problem in order to avoid unfeasible conditions for the solver in Aspen Plus. Specifically for the butyl acetate production process it was found that for the region with high methanol quality and low energy the NLP solver pushes the independent variables of the first distillation column (C1 reflux u_1 and distillate to feed u_2 ratios) to values that result in no liquid and/or vapor flow at certain stages in the column. Therefore resulting in major errors for the convergence in Aspen. Based on the preliminary results it was concluded that since the mass balances are not explicitly constraints for the optimization solver, and since in the original problem formulation there exist no constraint over any condition of the column C1, the solver tries to set the conditions of the tower towards a perfect separation of the mixtures MeAc/MeOH in the top and BuAc/BuOH in the bottom product. This condition drives the simulation very close to an infeasible region for convergence. To reduce this effect it was decided to impose two additional constraints on a minimum concentration (traces) of these products on the respective streams so the conditions of the column are kept in a feasible region.

5.3. Methanol production

For this process three objective functions were optimized, i.e., the carbon efficiency, total energy consumption and the profit. First, since the main purpose of this process is to treat the CO_2 present on the flue gas from combustion processes

Journal homepage: https://www.journals.elsevier.com/computers-and-chemical-engineering
Original file available at: https://www.sciencedirect.com/science/article/pii/S0098135417303198

(e.g. from electric power plants or thermal installations) and to produce an added value product, the carbon efficiency is critical to determine the extent of effectiveness of the process. The carbon efficiency is formulated as the ratio between carbon atoms that are converted to the added value product (i.e. CH_3OH) and the carbon atoms from the carbon source (i.e. CO_2 and CH_4). In Equation (15a) this objective is formulated as the ratio between the molar flow of these substances in the inlet streams and the top product of the distillation column. Other methanol molecules present in side streams (e.g. purge) as well as the unreacted material are considered losses. The second objective function evaluates the total energy demand per kmol of methanol produced, as established in Equation (15b).

Finally, the third objective function is a profit-cost function. This objective considers the income based on the methanol sales and the operational cost due to feedstock and the energy consumed. Additionally in this case the annualized capital cost (ann.CC) of the main units is considered since the operational conditions will determine the size and design requirements of these units. This objective is formulated according to Equation (16). Quality is not considered in this case as a parameter to define the product selling price. The product price is fixed based on its compliance with the quality specification, as it is established in the first constraint (Equation 17). The feedstock and energy costs are presented in Table 8, these values are taken from Zhang et al. (2013). The ann.CC is determined from the total capital cost (Total.CC) as described by Navarro-Amoros et al. (2014) considering a time horizon (n) of 10 years and an interest rate per year (i) of 8 %. To evaluate the capital cost only a subset of the units are considered. They are: compressors, methanol reactor and flash vessels. These units are considered as main contributors to the capital cost and these will be directly affected by the operational conditions evaluated in the optimization problem. The tri-reforming reactor is considered as well a main contribution to the capital cost of the process, however in this case a fixed capital cost is assumed since, contrary to the methanol reactor, the favorable conditions for kinetics and equilibrium of the tri-reforming process are both achieved at high temperatures. Moreover since it is a very fast reaction in the range of temperatures to be evaluated it can be assumed that the most favorable

Journal homepage: https://www.journals.elsevier.com/computers-and-chemical-engineering
Original file available at: https://www.sciencedirect.com/science/article/pii/S0098135417303198

conditions are governed by the reaction equilibrium. The boundaries established for the independent variables and the constraints on the optimization problem are formulated in Equation 17. The first three constraints guarantee a correct set of pressures in the process, with successively lower pressure for the two separators and the distillation column. The other two constraints set quality conditions for the products, i.e, methanol and water (diluted methanol).

$$J_1 = -\left(\frac{x_2}{u_1 + x_1}\right) \tag{15a}$$

$$J_2 = \frac{\sum_{i=5}^{19} |x_i|}{x_2/3600} \quad [MJ/kmol] \tag{15b}$$

$$J_3 = -\left(\text{income} - \text{costs} - \frac{\text{ann.cc}}{8000}\right) \quad [\$/h]$$

$$\begin{aligned}
\text{income} =& a_1 x_2 \\
\text{costs} =& a_2 u_1 + 3600 \times a_3(-x_{11} - x_{12} - x_{14} - x_{15} - x_{16} - x_{18}) + \\
& 3600 \times a_4(x_5 + x_7 + x_8 + x_9 + x_{19}) + a_5(x_6 + x_{17} + x_{13}) \\
\text{ann.CC} =& (Total.CC)\frac{i*(1+i)^n}{(1+i)^n - 1}; \qquad i = 0.08 \qquad n = 10 \\
& a_1 = 0.80 \qquad a_3 = 1 \times 10^{-10} \qquad a_5 = 8.98 \times 10^{-9} \\
& a_2 = 0.50 \qquad a_4 = 9 \times 10^{-5}
\end{aligned} \tag{16}$$

$$\begin{aligned}
& \min_{\mathbf{u} \in R^6} \quad [J_1,\, J_2,\, J_3] \\
\text{s.t.:} \quad & g_1(u) : 0 < u_6 - u_9 \leqslant 70 \qquad g_2(u) : 0 < u_9 - u_{10} \leqslant 25 \\
& g_3(u) : u_{13} - u_4 = 0 \qquad g_4(x) : 0.993 - x_3 \leqslant 0 \qquad g_5(x) : x_4 - 0.85 \leqslant 0 \\
& 200 < u_1 < 800 \qquad 1 < u_2 < 5 \qquad 400 < u_3 < 980 \\
& 50 < u_4, u_{13} < 300 \qquad 200 < u_5 < 300 \qquad 25 < u_6 < 40 \\
& 25 < u_7 < 50 \qquad 0.05 < u_8 < 0.3 \qquad 9 < u_9 < 30 \\
& 9 < u_{10} < 30 \qquad 1.5 < u_{11} < 3 \qquad 0.95 < u_{12} < 0.988
\end{aligned} \tag{17}$$

In Figure 13 the optimization results are depicted. In this case the reference conditions (+) are the optimal values reported for the same process by Zhang et al. (2013). As in the previous case studies the results of the MOO immediately point

Journal homepage: https://www.journals.elsevier.com/computers-and-chemical-engineering
Original file available at: https://www.sciencedirect.com/science/article/pii/S0098135417303198

out the potential process improvement compare to reference conditions, and therefore the significant added value of applying this optimization strategy. The numerical optimal solutions for the three objectives are presented in Table 13, together with the reference condition of the original process (Zhang et al., 2013). Regarding individual optimal solutions, the process shows a theoretical high potential to significantly improve the carbon efficiency obtained with the reference conditions. With a carbon efficiency of 96 %, this process has a enormous environmental potential. However apart from the optimal conditions in the methanol reactor and the process loop, the most significant contribution to achieve the high carbon efficiency is the use of an almost stoichiometric amount of methane for the tri-reforming. From a practical point of view these conditions can be undesired because they demand a very accurate control of the reactor conditions to guarantee the highest possible conversion of CO_2. In practice an small excess of methane could be fed into the reactor to guarantee the desired conversion. The profit (J_3) was maximized, reaching the highest value of 4733.5 [$/h] of economical benefit. However it has to be considered that a real value should be significantly lower due to the capital costs that were not considered because of their approximated constant character. Finally regarding energy, the minimum energy demand required by the process (J_2) is calculated to be 994.9 [MJ/kmol], which means a reduction of 26.6 % (360 [MJ/kmol]).

Similarly to what was found for the butyl acetate case, the convergence for this MOOP was obtained using NNC as scalarization method and two additional constraints were added to guarantee robustness for the model convergence in Aspen Plus. These constraints do not have a physical interpretation but help to avoid conditions that result on simulation errors in Aspen Plus. In this case, through preliminary studies, the distillation column was found as the most prone unit to generate errors. Therefore constraints were added to guarantee a minimum concentration of the trace components in both distillate and bottom products.

Finally, the detailed inspection of the Pareto front in Figure 13 shows that the system has a strong convex behavior on the Pareto front. In turn there exist strongly advantageous solutions that a decision maker could choose. Similar to

Journal homepage: https://www.journals.elsevier.com/computers-and-chemical-engineering
Original file available at: https://www.sciencedirect.com/science/article/pii/S0098135417303198

the profit-based MOO optimization for the butyl acetate case, the Pareto front shows a particular shape on the side of tradeoff points with minimum energy demand. Since these solutions are limited by a low energy consumption, they offer a moderate improvement on the carbon efficiency compare to the one obtained at the opposite side of the Pareto front. Therefore, starting from the points of minimum energy demand and maximum profit, there is a preferential path for rapidly increase on the carbon efficiency till a value around 93 % is achieved. This implies that there exist a region with tradeoff solutions that offer a significant improvement on the carbon efficiency keeping a relatively low energy demand and a high profit. One posible optimal solution in this region would be the one corresponding to 93.17 % carbon eficiency, 1033.8 [MJ/kmol] required energy and a profit estimated of 4024.2 [$/h]. This solution is significantly better than the reference conditions regarding the three objectives simultaneously, and it represents an improvement of 85.6, 89.2 and 63.8 % of the maximum potential improvement for each objective.

Regarding computational performance of the latter case studies, in Table 14 the computational time for each case study applying the developed gradient-based optimization interface is reported. All problems were solved with a laptop computer featuring an Intel ®$Core^{TM}$ i7-4500U at 2.40 GHz and 8 GB of RAM. The table shows the problem scale in each case. The scale is given by the model's size (i.e., in Aspen Plus the number of equations/dependent variables and number of independent variables), and the scale of the optimization problem which considers the number of degrees of freedom (i.e., a sub set of the independent variables in Aspen Plus) and the number of constraints. The number of Pareto points produced in the solution is taken into account to determine the average time spent per optimal point as an indicator of the computational performance. Even though the scale of the methanol case study is smaller in terms of number of equations in the simulation, the computational performance is slower. With 86.4 seconds per Pareto point it takes around three times longer than the butyl acetate case. This difference can be attributed to the model and optimization complexity. Even though the solution of the methanol case requires the convergence of less equations, it takes longer to the EO solver to find a solution. This is attributed to the system complexity which

Journal homepage: https://www.journals.elsevier.com/computers-and-chemical-engineering
Original file available at: https://www.sciencedirect.com/science/article/pii/S0098135417303198

includes two reactors, one of which depends on the total Gibbs free energy minimization algorithm of Aspen Plus. Additionally, the higher number of degrees of freedom results in a larger optimization problem, possibly with a higher computational effort if the constraints are highly nonlinear. Evidence of these elements can be found in the results reported by IPOPT regarding the time spent evaluating the objective functions and constraints (where the time required by Aspen Plus to converge is the major contributor) and the number of evaluations of these functions. While for the butyl acetate case the average time per evaluation is the 1.3 s, for the methanol case is 1.9 s. This clearly demonstrates the higher complexity for simulating the latter case study. Moreover, finding one Pareto point for the butyl acetate case required in average 13 evaluations while for the methanol case 37 were needed in average. This corresponding to the higher scale of the latter optimization problem.

These results demonstrate the key role that the model complexity in Aspen Plus plays for the computational performance of the optimization interface. Therefore it is difficult to establish the limiting scale for which the solution of the optimization problems becomes infeasible using the developed interface. Even for very large optimization problems with many degrees of freedom and constraints, results in acceptable computational time can be achieved if the model complexity in Aspen Plus is sufficiently low. This is possible due to the robustness of the CasADi - IPOPT framework. As an illustration of the computational efficiency of CasADi, Vallerio et al. (2016) have reported convergence time around 19 minutes for large scale dynamic optimization problems with 30 states 52,272 variables and 123,552 constraints.

6. Conclusion

Aspen and CasADi have been selected as the tools for computer-aided engineering in order to enable MOO in a flowsheet simulator. Two interfaces have been successfully constructed. The first one corresponds to approaches for *black box optimization* while the second one *accesses the ESO*. The former, based on vectorization methods, corresponds with the scheme that has been most commonly exploited in

Journal homepage: `https://www.journals.elsevier.com/computers-and-chemical-engineering`
Original file available at: `https://www.sciencedirect.com/science/article/pii/S0098135417303198`

the current state-of-art. It has been implemented to generate reference results for the first case study. The latter interface, based on scalarization methods is the main contribution of this paper. In addition the specific challenges of interfacing process simulators with optimization tools have been highlighted. The presented novel implementation allows gradient-based MOO of processes simulated with Aspen Plus, benefiting from the gradient information produced by the Aspen's EO engine.

Exploiting the gradient-based optimization results in a higher accuracy of the Pareto front and better capabilities to tackle constrained problems. Using the debutanizer column as a very intuitive case study with an illustrative objective function and a more realistic profit function, it has been possible to demonstrate the higher performance of this optimization approach. On the one hand, it demands, in the worse case similar computational time to the black box optimization, since fewer evaluations of the objective functions are required. And on the other hand it produces always more accurate and informative optimal solutions that serve to approximate the complete Pareto front. In terms of limitations of the developed optimization interface, these can be subdivided into two groups. On the one hand, some aspects are inherent to the MOO methods applied. This is illustrated in the debutanizer case study with the possibility of obtaining non-global optimal solutions and the tendency to produce non-optimal Pareto solutions. On the other hand, related directly to the architecture of the interface, the fact that the optimization accessing the ESO relies on a bi-level optimization scheme, where the system of flowsheet model equations is solved independently while in the upper level the MOO problem is solved based on those results, introduces uncertainty into the problem. Even though this limitation was surpassed in this contribution using NNC instead of NBI as scalarization method, this aspect could represent problems for other applications.

The developed tools have been illustrated with three relevant case studies, i.e., the debutanizer column, the butyl acetate process and the methanol production via tri-reforming. In all cases the Pareto front obtained proved to be very informative, providing beneficial tradeoffs for the optimization of each process. Specifically in the butyl acetate and methanol case studies, significant improvements with respect to

Journal homepage: https://www.journals.elsevier.com/computers-and-chemical-engineering
Original file available at: https://www.sciencedirect.com/science/article/pii/S0098135417303198

the current reference operating conditions have been observed. These results show that interfacing a process simulator for MOO can provide the process engineer with a better insight into the process conditions, while providing more alternatives to the decision maker. In future work the goal is to integrate the presented interface with interactive methods as discussed by Vallerio et al. (2015).

Acknowledgments

This work was supported by KU Leuven PFV/10/002 Center-of-Excellence Optimization in Engineering (OPTEC), CAM holds a VLAIO-Baekeland [HBC.2017.0239] grant, Fonds Wetenschappelijk Onderzoek Vlaanderen [G.0930.13] and the Belgian Science Policy Office (DYSCO) [IAP VII/19].

References

References

Ahmadi, A., Dehghani, O., Heravi, M., Rahimpour, M.R., 2015. Performance improvement and efficiency enhancement of a debutanizer column (a case study in South Pars gas field). *Journal of Natural Gas Science and Engineering*, 22:49–61.

Andersson, J., Akesson, J., Diehl, M., 2012. CasADi - a symbolic package for automatic differentiation and optimal control.In Proceedings of the 6th International Conference on Automatic Differentiation.

Ascher, U.M., Petzold, L.R., 1998. Computer methods for ordinary differential equations and differential-algebraic equations. *SIAM Journal*.

Aspen OOMF - Script Language Reference Manual, 2011. Aspen Technology, Inc.

Aspen Plus 2004.1 Getting Started Using Equation Oriented Modeling. Aspen Technology, Inc., 2005.

Bau, U., Neitzke, D., Lanzerath, F., Bardow, A., 2015. Multi-Objective Optimization of Dynamic Systems combining Genetic Algorithms and Modelica: Application to Adsorption Air-Conditioning Systems. *Proc.* 11^{th} *International Modelica Conference*, pages 777–784.

Journal homepage: `https://www.journals.elsevier.com/computers-and-chemical-engineering`
Original file available at: `https://www.sciencedirect.com/science/article/pii/S0098135417303198`

Bravo-Bravo, C., Segovia-Hernandez, J.G., Gutierrez A.C., Duran, A.L., Bonilla-Petriciolet, A., Briones-Ramirez, A., 2010. Extractive dividing wall column: design and optimization. *Industrial and Engineering Chemistry Research*, 49:3672-3688.

Bortz, M., Burger, J., Asprion, N., Blagov, S., Böttcher, R., Nowak, U., Scheithauer, A., Welke, R., Küfer, K.-H., Hasse, H., 2014. Multi-criteria optimization in chemical process design and decision support by navigation on Pareto sets. *Computers and Chemical Engineering*, 60:354–363.

Chen, W., Shao, Z., Qian, J., 2009. Interfacing ipopt with aspen open solvers and cape-open. In Oller, C.A., Brito Alves, R.M., Biscaia, E.C. (Eds.), *10th International Symposium on Process Systems Engineering: Part A*, volume 27 of *Computer Aided Chemical Engineering*, 201 – 206. Elsevier.

CO-LaN Consortium, 2003. CAPE-OPEN Open Interface Specification : Partial Differential Algebraic Equations Interface. *Cape-Open*.

Das, I., Dennis, J.E., 1998. Normal-Boundary Intersection: A new method for generating the Pareto surface in nonlinear multicriteria optimization problems. *SIAM Journal on Optimization*, 8:631–657.

Deb, K., Pratap, A., Agarwal, S., Meyarivan, T., 2002. A fast and elitist multiobjective genetic algorithm: NSGA-II. *IEEE Transaction on Evolutionary Computation*, 6:181–197.

Diaz, .M.S, Bandoni, .J.A., 1996. A mixed integer optimization strategy for a large scale chemicalplant in operation. *Computers and Chemical Engineering*, 20:531545.

Diwekar, U.M., Grossmann, I.E., Rubin, E.S., 1992. An MINLP process synthesizer for a sequential modular simulator. *Industrial and Engineering Chemistry Research*, 31:313322.

Eslick, J.C., David, C., Miller, D.C., 2011. A multi-objective analysis for the retrofit of a pulverized coal power plant with a CO2 capture and compression process. *Computers and Chemical Engineering*, 35(8):1488-1500.

Journal homepage: `https://www.journals.elsevier.com/computers-and-chemical-engineering`
Original file available at: `https://www.sciencedirect.com/science/article/pii/S0098135417303198`

Espie, D., Macchietto, S., 1989. The optimal design of dynamic experiments. AIChE Journal, 35:223–229.

Gangadwala, J., Kienle, A., 2007. MINLP optimization of butyl acetate synthesis. *Chemical Engineering and Processing: Process Intensification*, 46(2):107–118.

Geraili, A., Romagnoli, J.A., 2015. A multiobjective optimization framework for design of integrated biorefineries under uncertainty. *AIChE Journal*, 61(10):3208–3222.

Goldberg, D.E., 1989. Genetic algorithms in search, optimization, and machine learning. Addison-Wesley.

Gutirrez-Antonio, C., Briones-Ramrez, A., 2009. Pareto front of ideal Petlyuk sequences using a multiobjective genetic algorithm with constraints. *Computers and Chemical Engineering*, 33:454-464.

Hakanen, J., Hakala, J., Manninen, J., 2006. An integrated multiobjective design tool for process design. *Applied Thermal Engineering*, 26(13):1393–1399.

Harsh, M.G., Saderne, P., Biegler, L.T., 1989. A mixed integer flowsheet optimization strategy for process retrofits-the debottlenecking problem. *Computers and Chemical Engineering*, 13:94757.

Jang, W.H., Hahn, J., Hall, K.R., 2005. Genetic/quadratic search algorithm for plant economic optimizations using a process simulator. *Computers and Chemical Engineering*, 30(2):285–294.

Jimenez, L., Garvin, A., Costa-Lopez, J., 2002. The Production of Butyl Acetate and Methanol via Reactive and Extractive Distillation II. Process Modeling, Dynamic Simulation and Control Strategy. *Industrial and Engineering Chemistry Research*, 41:6735–6744.

Kim, H., Kim, I.H., Yoon, E.S., 2010. Multiobjective Design of Calorific Value Adjustment Process using Process Simulators. *Industrial & Engineering Chemistry Research*, 49(6):2841–2848.

Journal homepage: `https://www.journals.elsevier.com/computers-and-chemical-engineering`
Original file available at: `https://www.sciencedirect.com/science/article/pii/S0098135417303198`

Lang, Y.-D., Biegler, L.T., 2005. Large-Scale Nonlinear Programming with a CAPE-OPEN Compliant Interface. *Chemical Engineering Research and Design*, 83(6):718–723.

Lang, Y.-D., Biegler, L.T., 2007. A software environment for simultaneous dynamic optimization. *Computers and Chemical Engineering*, 31(8):931–942.

Leineweber, D.B., Bauer, I., Bock, H.G., Schlöder, J.P., 2003. An efficient multiple shooting based reduced SQP strategy for large-scale dynamic process optimization. Part 1: Theoretical aspects. *Computers and Chemical Engineering*, 27(2):157–166.

Liu, Z., Huang, Y., 2012. Technology evaluation and decision making for sustainability enhancement of industrial systems under uncertainty. AIChE Journal, 58(6):1841–1852.

Logist, F., Houska, B., Diehl, M., Van Impe, J., 2010. Fast pareto set generation for nonlinear optimal control problems with multiple objectives. *Structural and Multidisciplinary Optimization*, 42:591–603.

Logist, F., Telen, D., Houska, B., Diehl, M., Van Impe, J., 2013. Multi-objective optimal control of dynamic bioprocesses using ACADO toolkit. *Bioprocess and Biosystems Engineering*, 36(2):151–164.

Logist, F., Van Erdeghem, P., Van Impe, J., 2009. Efficient deterministic multiple objective optimal control of (bio)chemical processes. Chemical Engineering Science, 64:2527-2538.

Luyben, W.L., Pszalgowski, K.M., Schaefer, M.R., Siddons, C., 2004. Design and Control of Conventional and Reactive Distillation Processes for the Production of Butyl Acetate. *Industrial and Engineering Chemistry Research*, 43:8014–8025.

Luyben, W.L., 2010. Design and Control of a Methanol Reactor/Column Process. *Industrial and Engineering Chemistry Research*, 49:6150-6163.

Luyben, W.L., 2011. Principles and Case Studies of Simultaneous Design. WILEY.

Journal homepage: `https://www.journals.elsevier.com/computers-and-chemical-engineering`
Original file available at: `https://www.sciencedirect.com/science/article/pii/S0098135417303198`

Messac, A., Ismail-Yahaya, A., Mattson, C.A., 2003. The normalized normal constraint method for generating the Pareto frontier. *Structural and Multidisciplinary Optimization*, 25(2):86–98.

Miettinen, K., 1999. Nonlinear multiobjective optimization. Kluwer Academic Publishers, Boston.

Nakayama, H., Yun, Y., Yoon, M., 2009. Sequential Approximate Multiobjective Optimization Using Computational Intelligence, Springer Berlin Heidelberg.

Navarro-Amors, M.A., Ruiz-Femenia, R., Caballero, J.A., 2014. Integration of modular process simulators under the Generalized Disjunctive Programming framework for the structural flowsheet optimization. *Computers and Chemical Engineering*, 67:1325.

Nocedal, J., Stephen, J.W., 1999. Numerical Optimization, second ed. Springer.

Ramzan, N., Witt, W., 2006. Multi-objective optimization in distillation unit: a case study. *Canadian Journal of Chemical Engineering*, 84(5):604–613.

Rangaiah, G.P., Bonilla-Petricolet, A, 2013. Multi-Objective Optimization in Chemical Engineering-Developments and Applications, First Ed. Wiley.

Ren, J., Xu, D., Cao, H., Wei, S., Dong, L., Goodsite, M.E., 2016. Sustainability decision support framework for industrial system prioritization. AIChE Journal, 62(1):108–130.

Sadrieh, A., Bahri, P.A., 2011. Optimal Control of the Process Systems Using Graphic Processing Unit. IFAC Proceedings Volumes. 44(1):12108–12113.

Schopfer, G., Wyes, J., Marquardt, W., Von Wedel, L., 2005. A library for equation system processing based on the CAPE-OPEN ESO Interface. *Computer Aided Chemical Engineering*, 20(C):1573–1578.

Song, C., Pan, W., 2004. Trireforming of methane: A novel concept for catalytic production of industrially useful synthesis gas with desired H_2/CO ratios. *Catalysis Today*, 98:463–484.

Srinivas, N., Deb, K., 1994. Multiobjective function optimization using nondominated sorting genetic algorithms. *Evolutionary Computation Journal*, 2:221–248.

Journal homepage: `https://www.journals.elsevier.com/computers-and-chemical-engineering`
Original file available at: `https://www.sciencedirect.com/science/article/pii/S0098135417303198`

Steinigeweg, S., Gmehling, J., 2004. Transesterification processes by combination of reactive distillation and pervaporation. *Chemical Engineering and Processing: Process Intensification*, 43(3):447 – 456.

Tang, Y.-T., Chen, Y-W., Huang, H.-P., Yu, C.-C., Hung, S.-B., Lee, M.-J., 2005. Design of reactive distillations for acetic acid esterification. *AIChE Journal*, 51(6):1683–1699.

Tarafder, A., Rangaiah, G.P., Ray, A.K., 2005. Multiobjective optimization of an industrial styrene monomer manufacturing process. *Chemical Engineering Science*, 60:347–363.

Taras, S., Woinaroschy, A., 2012. An interactive multi-objective optimization framework forsustainable design of bioprocesses. *Computers and Chemical Engineering*, 43:10-22.

Telen, D., Logist, F., Quirynen, R., Houska, B., Diehl, M., Van Impe, J., 2014. Optimal experiment design for nonlinear dynamic (bio)chemical systems using sequential semidefinite programming. AIChE Journal, 60:1728–1739.

Vallerio, M., Vercammen, D., Van Impe, J., Logist, F., 2015. Interactive NBI and (E)NNC methods for the progressive exploration of the criteria space in multi-objective optimization and optimal control. Computers and Chemical Engineering, 82:186–201.

Vallerio, M., Telen, D., Cabianca, L., Maneti, Flavio., Van Impe, J., Logist, F., 2016. Robust multi-objective dynamic optimization of chemical processes using the Sigma Point method. Chemical Engineering Science, 140:201–216.

Van Derlinden, E., Bernaerts, K., Van Impe, J., 2010. Simultaneous versus sequential optimal experiment design for the identification of multi-parameter microbial growth kinetics as a function of temperature. Journal of Theoretical Biology, 264:347–355.

Verheyden, F., 2014. Exergy analysis and optimization of transesterification reaction: butyl acetate case. Master Thesis. KU Leuven.

Journal homepage: `https://www.journals.elsevier.com/computers-and-chemical-engineering`
Original file available at: `https://www.sciencedirect.com/science/article/pii/S0098135417303198`

Wächter, A., Biegler, L.T., 2006. On the implementation of a primal-dual interior point filter line search algorithm for large-scale nonlinear programming. Mathematical Programming, 106(1):25–57.

Wang, D., Feng, X., 2013. Simulation and multi-objective optimization of an integrated process for hydrogen production from refinery off-gas. *International Journal of Hydrogen Energy*, 38(29):12968–12976.

Wang, S.J., Wong, D.S.H., Yu, S.W., 2008. Design and control of transesterification reactive distillation with thermal coupling. *Computers and Chemical Engineering*, 32(12):3030 – 3037.

White, D.C., 2012. Optimize Energy Use in Distillation. *CEP Magazine, AIChE.*

Zhang, Y., Cruz, J., Zhang, S., Lou, H.H., Benson, T.J. 2013. Process simulation and optimization of methanol production coupled to tri-reforming process. *International Journal of hydrogen energy*, 38:13617 – 13630.

Journal homepage: `https://www.journals.elsevier.com/computers-and-chemical-engineering`
Original file available at: `https://www.sciencedirect.com/science/article/pii/S0098135417303198`

Tables

Compound/Fraction	**wt%**
Propene (225.55 K)	1.2
Propane (230.95 K)	3.2
Isobutane (260.15 K)	0.5
Butane (272.15 K)	2.3
Butenes (266.68 K)	1.8
C_5 - 453.15 K	81.8
453.15 K - 623.15 K	9.2

Table 1: Feed composition for the debutanizer column.

Journal homepage: https://www.journals.elsevier.com/computers-and-chemical-engineering
Original file available at: https://www.sciencedirect.com/science/article/pii/S0098135417303198

Parameter	Value	Units
Feed Temperature	441.15	K
Feed Pressure	1.52	MPa
Feed Mass Flow	38.3	kg/s
Number of stages	16	-
Feed stage	7	-
Pressure at condenser	1.1	MPa
Degrees subcooled	288.15	K

Table 2: Process conditions and fixed parameters for the debutanizer column optimization.

Journal homepage: https://www.journals.elsevier.com/computers-and-chemical-engineering
Original file available at: https://www.sciencedirect.com/science/article/pii/S0098135417303198

Variable	Optimization	Simulation	Units
Controls	u_1	Mass reflux ratio	-
	u_2	Distillate mass flow	kg/s
States	x_1	Reboiler duty	MW
	x_2	Condenser duty	MW
	x_3	C_5 *wt* fraction in distillate	-
	x_4	Bottoms mass flow	kg/s
	x_5	Isobutane *wt* fraction in bottoms	-
	x_6	Butane *wt* fraction in bottoms	-
	x_7	Butene *wt* fraction in bottoms	-
	x_8	Feed mass flow	kg/s

Table 3: Description of the model states and control variables for the debutanizer.

Journal homepage: `https://www.journals.elsevier.com/computers-and-chemical-engineering`
Original file available at: `https://www.sciencedirect.com/science/article/pii/S0098135417303198`

Parameter		Value	Units
Feed 1 (MeAc)	Pressure	1.013	MPa
	Temperature	305	K
	Flow	100	kmol/h
	MeAc	0.6	Mole-frac.
	MeOH	0.4	Mole-frac.
Feed 2 (BuOH)	Pressure	1.013	MPa
	Temperature	305	K
	Flow	59.4	kmol/h
	BuOH	1.0	Mole-frac.
Reactor	Temperature	350	K
C1	Num. stages	37	-
	Cond. Pressure	0.122	MPa
C2	Num. stages	27	-
	Cond. Pressure	0.111	MPa
C3	Num. stages	47	-
	Cond. Pressure	0.405	MPa

Table 4: Process conditions and fixed parameters to model and optimize the butyl acetate production process.

Journal homepage: https://www.journals.elsevier.com/computers-and-chemical-engineering
Original file available at: https://www.sciencedirect.com/science/article/pii/S0098135417303198

Variable	Optimization	Simulation	Units
Controls	u_1	Reflux ratio C1	-
	u_2	Distillate to feed ratio C1	-
	u_3	Reflux ratio C2	-
	u_4	Distillate to feed ratio C2	-
	u_5	Reflux ratio C3	-
	u_6	Distillate to feed ratio C3	-
States	x_1	B4 Heat duty	MW
	x_2	B5 Cooling duty	MW
	x_3	CSTR Cooling duty	MW
	x_4	B10 Heat duty	MW
	x_5	C1 Reboiler duty	MW
	x_6	C1 Condenser duty	MW
	x_7	B11 Heat duty	MW
	x_8	P9 Work duty	MW
	x_9	B12 Heat duty	MW
	x_{10}	C2 Reboiler duty	MW
	x_{11}	C2 Condenser duty	MW
	x_{12}	C3 Reboiler duty	MW
	x_{13}	C3 Condenser duty	MW
	x_{14}	P6 Work duty	MW
	x_{15}	P3 Work duty	MW
	x_{16}	Methanol purity (B2)	Mole frac.
	x_{17}	Butyl acetate purity (B3)	Mole frac.
	x_{18}	Molar flow distillate C2	kmol/s
	x_{19}	Molar flow distillate C3	kmol/s
	x_{20}	Mass flow methanol produced	kg/h
	x_{21}	Mass flow butyl acetate produced	kg/h
	x_{22}	Mass flow butanol (inlet)	kg/h

Table 5: Optimization variables designation for MOO of the butyl acetate process.

Journal homepage: `https://www.journals.elsevier.com/computers-and-chemical-engineering`
Original file available at: `https://www.sciencedirect.com/science/article/pii/S0098135417303198`

Parameter		Value	Units
CH4	Pressure	0.101	MPa
	Temperature	298.15	K
	CH_4	1.0	Mole-frac.
Fluegas	Pressure	0.101	MPa
	Temperature	423.15	K
	Flow	1000	kmol/h
	CO_2	0.1	Mole-frac.
	O_2	0.03	Mole-frac.
	N_2	0.67	Mole-frac.
	H_2O	0.2	Mole-frac.
Dist. Column	Num. stages	19	-

Table 6: Process conditions and fixed parameters to model and optimize the methanol production process.

Journal homepage: https://www.journals.elsevier.com/computers-and-chemical-engineering
Original file available at: https://www.sciencedirect.com/science/article/pii/S0098135417303198

Variable	Optimization	Simulation	Units
Controls	u_1	Methane molar flow (inlet)	kmol/h
	u_2	Pressure reforming reactor	MPa
	u_3	Temperature reforming reactor	K
	u_4	Pressure methanol reactor	MPa
	u_5	Temperature methanol reactor	K
	u_6	Pressure Separator 1	MPa
	u_7	Temperature Separator 1	K
	u_8	Purge fraction	-
	u_9	Pressure Separator 2	MPa
	u_{10}	Pressure dist. column	MPa
	u_{11}	Reflux ratio dist. column	-
	u_{12}	Distillate - feed ratio dist. column	-
	u_{13}	Discharge pressure recycle compressor	MPa
States	x_1	CO_2 molar flow (fluegas)	kmol/h
	x_2	CH_4O flow (methanol)	kmol/h
	x_3	CH_4O purity (methanol)	Mole-frac.
	x_4	CH_4O fraction (water)	Mole-frac.
	x_5	In-pre work duty	MW
	x_6	H-1 Heat duty	MW
	x_7	Press-1 work duty	MW
	x_8	Press-2 work duty	MW
	x_9	Press-3 work duty	MW
	x_{10}	H-2 Heat duty	MW
	x_{11}	C-2 Heat duty	MW
	x_{12}	Dist. condenser duty	MW
	x_{13}	Dist. reboiler duty	MW
	x_{14}	C-1 Heat duty	MW
	x_{15}	C1 Heat duty	MW
	x_{16}	C2 Heat duty	MW
	x_{17}	Reforming reactor heat duty	MW
	x_{18}	Methanol reactor heat duty	MW
	x_{19}	Recycle comp. work duty	MW
	x_{20}	CO conc. MeOH reactor	Mole frac.
	x_{21}	CO_2 conc. MeOH reactor	Mole frac.
	x_{22}	H_2 conc. MeOH reactor	Mole frac.
	x_{23}	H_2O conc. MeOH reactor	Mole frac.
	x_{24}	CH_4O conc. MeOH reactor	Mole frac.
	x_{25}	Equilibrium constant RX Eq.7a	-
	x_{26}	Equilibrium constant RX Eq.7b	-
	x_{27}	H_2 converted MeOH reactor	kmol/h
	x_{28}	Actual vol. gas flow Separator 1	m^3/h
	x_{29}	Actual vol. gas flow Separator 2	m^3/h

Table 7: Optimization variables designation for MOO of the methanol process.

Journal homepage: `https://www.journals.elsevier.com/computers-and-chemical-engineering`
Original file available at: `https://www.sciencedirect.com/science/article/pii/S0098135417303198`

Postprint version of paper published in Computers & Chemical Engineering 2018, vol.109, p. 119-137.
The content is identical to the published paper, but without the final typesetting by the publisher.

Item		Specification	Price
Chemicals	Methanol	$\geq$ 99.5 wt % pure	0.8 ($/kg)
	Methane	$\geq$ 99 mol % pure	0.5 ($/kg)
Utilities	Cooling water	4,184 J/kg	0.1 ($/GJ)
	Electricity	-	0.09($/kWhr)
	Heat	55,688 kJ/kg	0.5 ($/kg)

Table 8: Chemicals and utilities prices for profit evaluation

Journal homepage: https://www.journals.elsevier.com/computers-and-chemical-engineering
Original file available at: https://www.sciencedirect.com/science/article/pii/S0098135417303198

Postprint version of paper published in Computers & Chemical Engineering 2018, vol.109, p. 119-137.
The content is identical to the published paper, but without the final typesetting by the publisher.

Results		Optimization accessing ESO States linearization	Embedded state function	Black box optimization
Convergence time [min]		0.61	0.72	1.35
Controls	u_1	23.88	23.85	21.95
	u_2	10679	10679	10640
Objective function		-557.76	-557.71	-497.39
Constraint		0	0	$1.69 \cdot 10^{-4}$

Table 9: Results for the optimization of the ilustrative objective function for the debutanizer column, subject to the quality constraint.

Journal homepage: `https://www.journals.elsevier.com/computers-and-chemical-engineering`
Original file available at: `https://www.sciencedirect.com/science/article/pii/S0098135417303198`

Convergence time [min]	Optimization accessing ESO States linearization	Embedded state function	Black box optimization
Bi-objective 16 Pareto points	2.99	3.73	3.47
Tri-objective 45 Pareto points	9.38	10.51	2.41

Table 10: Convergence time for bi and tri objective optimization problems for the debutanizer column using the ilustrative function.

Journal homepage: https://www.journals.elsevier.com/computers-and-chemical-engineering
Original file available at: https://www.sciencedirect.com/science/article/pii/S0098135417303198

Results		Total energy demand minimized	Total recycle flow minimized	Methanol quality maximized	Profit maximized	Original process Luyben (2011)	
Controls	u_1	0.2400	0.2968	0.3793	0.3149	0.3170	-
	u_2	0.5883	0.5739	0.5904	0.5915	0.6119	-
	u_3	1.0758	1.2000	1.0542	0.9820	0.9960	-
	u_4	0.5407	0.5000	0.6333	0.6021	0.6199	-
	u_5	2.6971	3.8000	2.4588	2.5304	1.9200	-
	u_6	0.6657	0.6560	0.6842	0.6562	0.6946	-
Objective functions	J_1	20.0699	21.4196	24.3717	21.7163	22.2840	MW
	J_2	0.0643	0.0579	0.0838	0.0735	0.0818	kmol/s
	J_3	-0.9280	-0.9280	-0.9960	-0.9951	-0.9284	(-)mole frac.
	J_4	-3411	-3398	-5419	-5463	-3375	(-)$/h

Table 11: Results for the multi-objective optimization of the butyl acetate production process.

Journal homepage: https://www.journals.elsevier.com/computers-and-chemical-engineering
Original file available at: https://www.sciencedirect.com/science/article/pii/S0098135417303198

IPOPT options	Debutanizer		Butyl Acetate	Methanol
	Illustrative case	Profit MOO		
Convergence tol.	1×10^{-5}	def.	1×10^{-5}	1×10^{-5}
Dual infeasibility tol.	def.	def.	1.5	1×10^{-5}
Constraint violation tol.	def.	def.	1×10^{-3}	1×10^{-5}
Complementarity tol.	def.	def.	1×10^{-3}	1×10^{-5}
Acceptable iter.	5	def.	3	3
Accep. convergence tol.	0.05	def.	0.5/5	5×10^{-3}
Accep. dual inf. tol.	0.05	def.	0.5/5	5×10^{-3}
Accep. constraint vio. tol.	1×10^{-3}	def.	5×10^{-3}	1×10^{-4}
Accep. Complementarity tol.	1×10^{-2}	def.	1×10^{-4}	1×10^{-4}
Accep Obj. change tol.	1×10^{-3}	def.	5×10^{-3}	5×10^{-2}
Hessian approximation	limited-memory			
Linear solver	MUMPS			
Pivot tolerance	default: 1e-6			

Table 12: IPOPT options used for the solution of the case studies.

Journal homepage: `https://www.journals.elsevier.com/computers-and-chemical-engineering`
Original file available at: `https://www.sciencedirect.com/science/article/pii/S0098135417303198`

Results		Carbon effic. maximized	Total energy demand minimized	Profit maximized	Original process Zhang et al. (2013)	
Controls	u_1	345.93	378.80	365.19	400.00	kmol/h
	u_2	1.0000	3.7428	2.1283	1.0000	MPa
	u_3	980.00	942.96	980.00	850.00	K
	u_4	300.00	173.76	50.000	50.000	MPa
	u_5	200.00	200.00	200.00	220.00	K
	u_6	40.000	31.804	40.000	24.000	MPa
	u_7	25.000	31.617	25.000	25.000	K
	u_8	0.0500	0.3000	0.0500	0.0500	-
	u_9	9.1178	9.0000	12.750	10.000	MPa
	u_{10}	9.0000	9.0000	12.750	10.000	MPa
	u_{11}	3.0000	1.5000	1.5000	1.5000	-
	u_{12}	0.9880	0.9880	0.9888	0.9888	-
	u_{13}	300.00	173.76	50.000	50.000	MPa
Objective functions	J_1	-0.9604	-0.8483	-0.8693	-0.7617	(-effc.)
	J_2	1566.9	994.9	1150.5	1354.9	[MJ/kmol]
	J_3	-931.5	-4269.0	-4733.5	-2771.2	[(-)$/h].

Table 13: Results for the multi-objective optimization of the methanol production process.

Journal homepage: `https://www.journals.elsevier.com/computers-and-chemical-engineering`
Original file available at: `https://www.sciencedirect.com/science/article/pii/S0098135417303198`

MOO Problem		Problem scale				Number Pareto pints	Total time [min]	Time per Pareto point [min]
		Simulation		Optimization				
		# Eq.	Ind. var.	deg. of freedom	const.			
Butyl acetate	Quality-based	2919	169	6	6	28	13	0.46
	Profit-based	2919	169	6	6	28	14.4	0.52
Methanol via tri-reforming		1572	306	13	7	15	21.6	1.44

Table 14: Computational performance for the MOO of the butyl acetate and methanol processes.

Journal homepage: `https://www.journals.elsevier.com/computers-and-chemical-engineering`
Original file available at: `https://www.sciencedirect.com/science/article/pii/S0098135417303198`

Figures

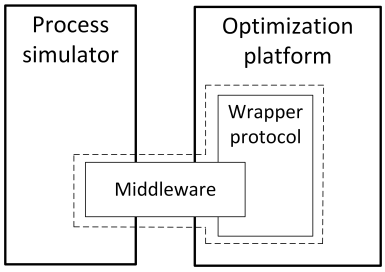

Figure 1: Concept of the interface architecture.

Journal homepage: https://www.journals.elsevier.com/computers-and-chemical-engineering
Original file available at: https://www.sciencedirect.com/science/article/pii/S0098135417303198

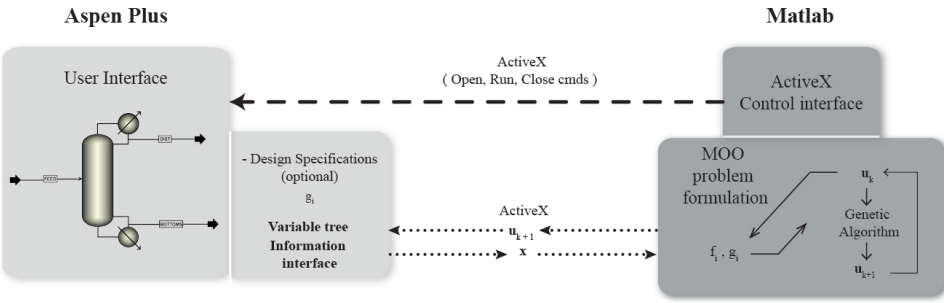

Figure 2: Scheme of the interface constructed for black box optimization exploiting a genetic algorithm in Matlab.

Journal homepage: `https://www.journals.elsevier.com/computers-and-chemical-engineering`
Original file available at: `https://www.sciencedirect.com/science/article/pii/S0098135417303198`

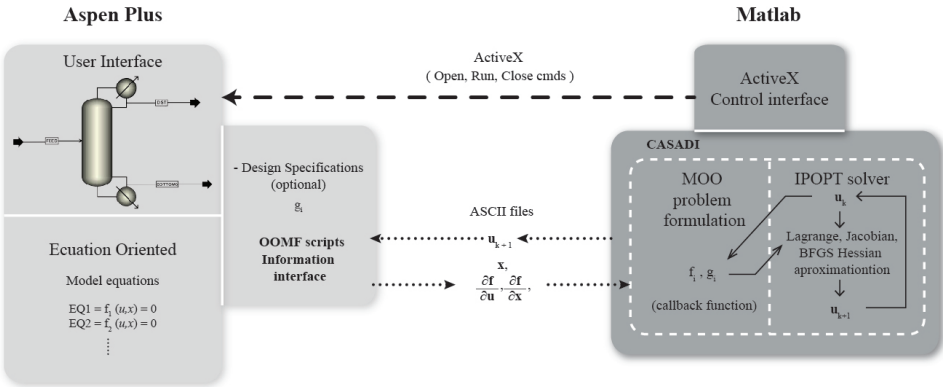

Figure 3: Scheme of the interface constructed for optimization accessing the ESO exploiting gradient-based optimization algorithms of CasADi for Matlab.

Journal homepage: `https://www.journals.elsevier.com/computers-and-chemical-engineering`
Original file available at: `https://www.sciencedirect.com/science/article/pii/S0098135417303198`

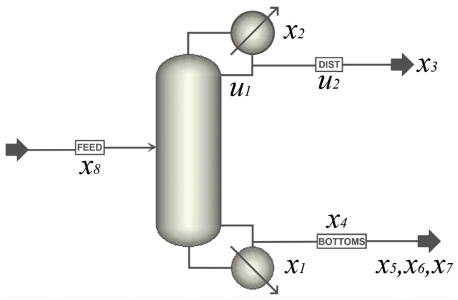

Figure 4: Debutanizer column with decision variables and model states.

Journal homepage: https://www.journals.elsevier.com/computers-and-chemical-engineering
Original file available at: https://www.sciencedirect.com/science/article/pii/S0098135417303198

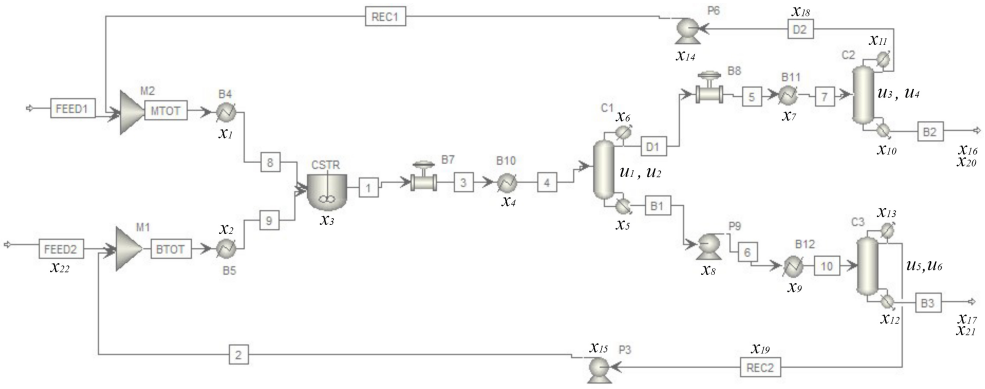

Figure 5: Traditional butyl acetate production process Luyben et al. (2004).

Journal homepage: `https://www.journals.elsevier.com/computers-and-chemical-engineering`
Original file available at: `https://www.sciencedirect.com/science/article/pii/S0098135417303198`

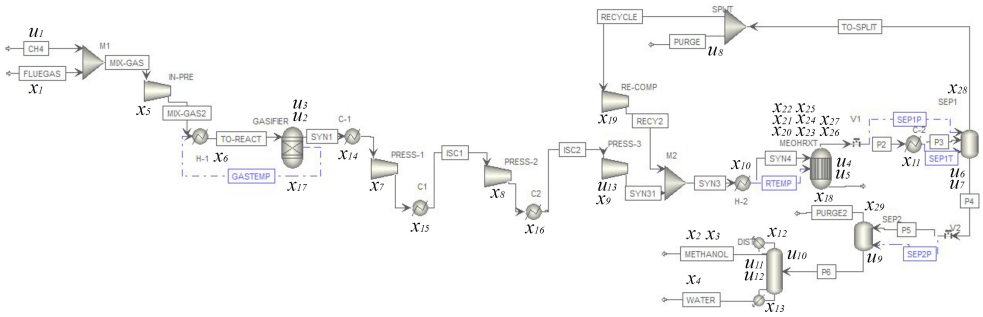

Figure 6: Methanol production process via tri-reforming.

Journal homepage: `https://www.journals.elsevier.com/computers-and-chemical-engineering`
Original file available at: `https://www.sciencedirect.com/science/article/pii/S0098135417303198`

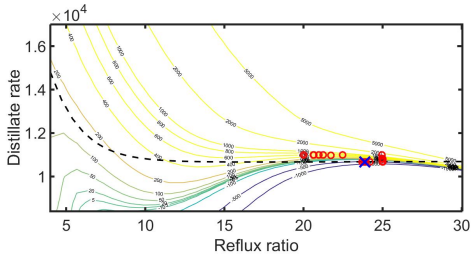

(a) Best known optimal solution for ESO approach.

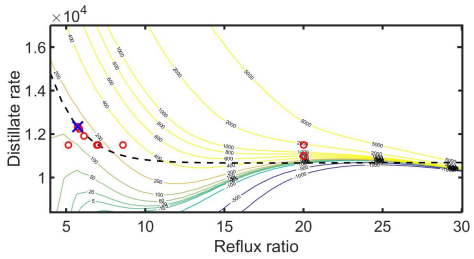

(b) Local optimal solution for the ESO approach.

Figure 7: Convergence to different optimal points in a ilustrative objective function - optimization accessing the ESO for the debutanizer column.

Journal homepage: `https://www.journals.elsevier.com/computers-and-chemical-engineering`
Original file available at: `https://www.sciencedirect.com/science/article/pii/S0098135417303198`

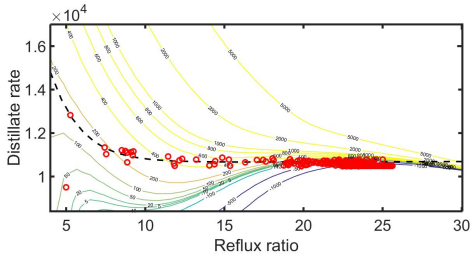

(a) Unsuccessful black box optimization.

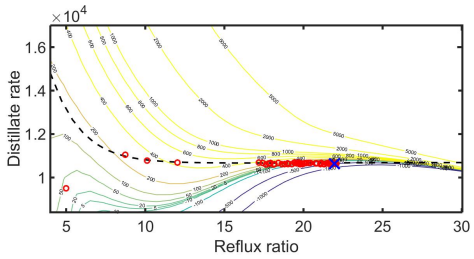

(b) Black box optimization.

Figure 8: Convergence issues when problem must cope with constraints - black box optimization for the debutanizer column.

Journal homepage: `https://www.journals.elsevier.com/computers-and-chemical-engineering`
Original file available at: `https://www.sciencedirect.com/science/article/pii/S0098135417303198`

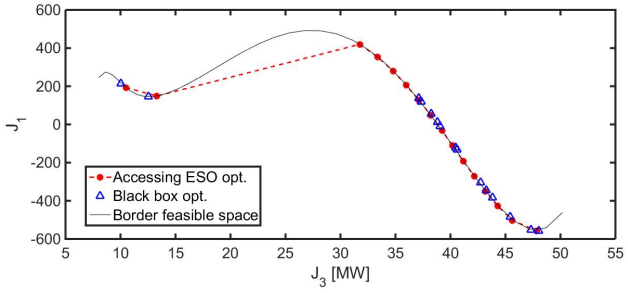

Figure 9: Comparison of the obtained Pareto front in the bi-objective optimization case for the debutanizer column.

Journal homepage: `https://www.journals.elsevier.com/computers-and-chemical-engineering`
Original file available at: `https://www.sciencedirect.com/science/article/pii/S0098135417303198`

Postprint version of paper published in Computers & Chemical Engineering 2018, vol.109, p. 119-137.
The content is identical to the published paper, but without the final typesetting by the publisher.

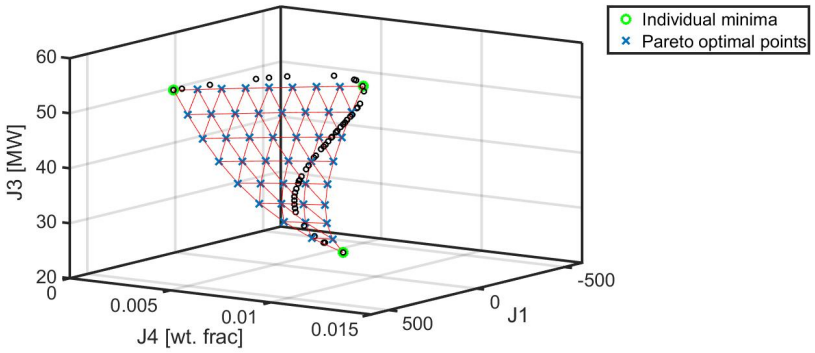

Figure 10: Comparison of the Pareto front obtained via ESO approach (x) and black box optimization (black o) for the debutanizer column.

Journal homepage: `https://www.journals.elsevier.com/computers-and-chemical-engineering`
Original file available at: `https://www.sciencedirect.com/science/article/pii/S0098135417303198`

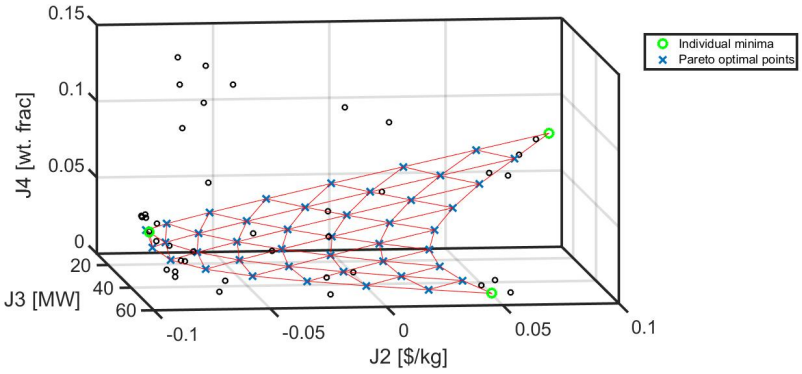

Figure 11: Pareto front for the profit-energy-quality optimization of the debutanizer column via ESO approach (x) and black box optimization (o).

Journal homepage: `https://www.journals.elsevier.com/computers-and-chemical-engineering`
Original file available at: `https://www.sciencedirect.com/science/article/pii/S0098135417303198`

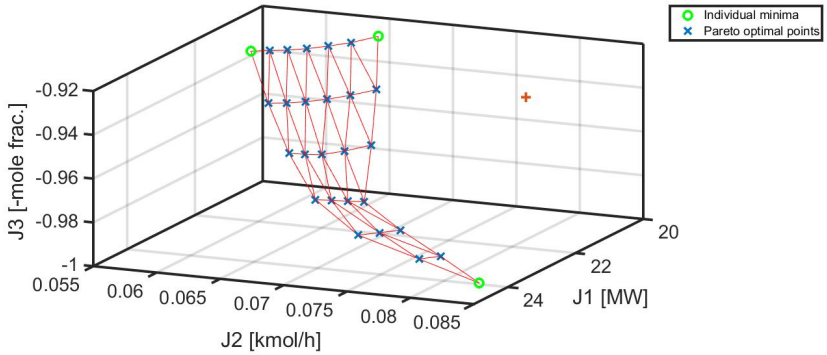

(a) Quality-based MOO.

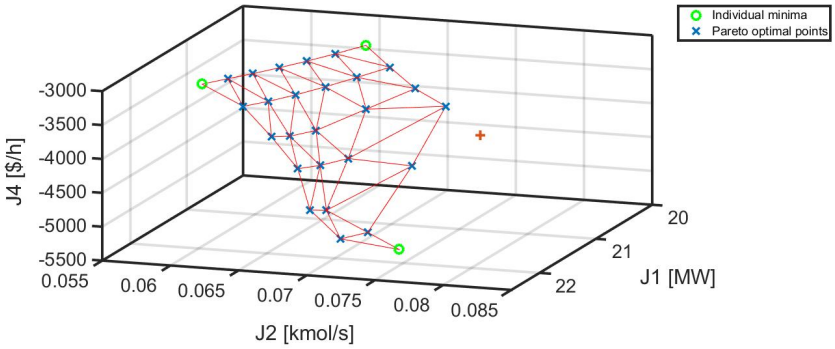

(b) Profit-based MOO.

Figure 12: Pareto front via ESO approach for MOO of the butyl acetate production process.

Journal homepage: `https://www.journals.elsevier.com/computers-and-chemical-engineering`
Original file available at: `https://www.sciencedirect.com/science/article/pii/S0098135417303198`

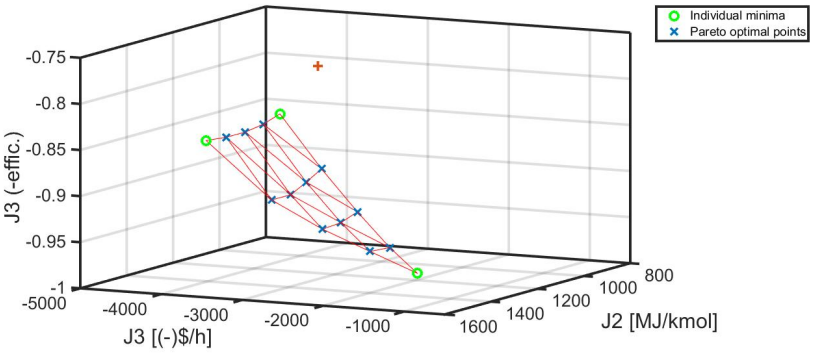

Figure 13: Pareto front via ESO approach for the carbon efficiency-energy-profit optimization of the methanol production via tri-reforming.

Journal homepage: `https://www.journals.elsevier.com/computers-and-chemical-engineering`
Original file available at: `https://www.sciencedirect.com/science/article/pii/S0098135417303198`